CONTRACTOR REPORT ARCCB-CR-94004

A REVIEW OF RADIAL FORGING TECHNOLOGY INCLUDING PREFORM DESIGN FOR PROCESS OPTIMIZATION

JOSEPH P. DOMBLESKY
RAJIV SHIVPURI
TAYLAN ALTAN

THE OHIO STATE UNIVERSITY
COLUMBUS, OHIO 43210

FEBRUARY 1994

US ARMY ARMAMENT RESEARCH,
DEVELOPMENT AND ENGINEERING CENTER
CLOSE COMBAT ARMAMENTS CENTER
BENÉT LABORATORIES
WATERVLIET, N.Y. 12189-4050

DISCLAIMER

The findings in this report are not to be construed as an official Department of the Army position unless so designated by other authorized documents.

The use of trade name(s) and/or manufacturer(s) does not constitute an official indorsement or approval.

DESTRUCTION NOTICE

For classified documents, follow the procedures in DoD 5200.22-M, Industrial Security Manual, Section II-19 or DoD 5200.1-R, Information Security Program Regulation, Chapter IX.

For unclassified, limited documents, destroy by any method that will prevent disclosure of contents or reconstruction of the document.

For unclassified, unlimited documents, destroy when the report is no longer needed. Do not return it to the originator.

REPORT DOCUMENTATION PAGE

Form Approved
OMB No. 0704-0188

1. AGENCY USE ONLY (Leave blank)	2. REPORT DATE	3. REPORT TYPE AND DATES COVERED
	February 1994	Final

4. TITLE AND SUBTITLE
A REVIEW OF RADIAL FORGING TECHNOLOGY INCLUDING PREFORM DESIGN FOR PROCESS OPTIMIZATION

5. FUNDING NUMBERS
Contract DAAA22-89-M-0081

6. AUTHOR(S)
Joseph P. Domblesky, Rajiv Shivpuri, and
Taylan Altan

7. PERFORMING ORGANIZATION NAME(S) AND ADDRESS(ES)
NSF Engineering Research Center
for Net Shape Manufacturing
The Ohio State University
Columbus, Ohio 43210

8. PERFORMING ORGANIZATION REPORT NUMBER

9. SPONSORING / MONITORING AGENCY NAME(S) AND ADDRESS(ES)
U.S. Army ARDEC
Benet Laboratories, SMCAR-CCB-TL
Watervliet, NY 12189-4050

10. SPONSORING / MONITORING AGENCY REPORT NUMBER
ARCCB-CR-94004

11. SUPPLEMENTARY NOTES
Charles Calderone - Benet Laboratories Project Engineer

12a. DISTRIBUTION / AVAILABILITY STATEMENT
Approved for public release; distribution unlimited.

12b. DISTRIBUTION CODE

13. ABSTRACT (Maximum 200 words)

The Engineering Research Center for Net Shape Manufacturing (located at Ohio State University, Columbus, Ohio) was contracted by Benet Laboratories to investigate the rotary forging operation at Watervliet Arsenal. They were asked to make recommendations on how to optimize the shape and size of the starting material (preform) prior to forging which would reduce or eliminate variations in mechanical properties along the length of the resulting forging. Based on the data supplied by Benet Laboratories, the study resulted in recommendation of a two-step preform design. This was a preliminary recommendation and further testing was suggested to separate the effects of forging reduction from post-forging heat treatment.

14. SUBJECT TERMS	15. NUMBER OF PAGES
Deformation Zones, Forging Reduction, Heat Treatment, Mechanical Properties, Optimization, Preform, Rotary Forging, Strain Rates	106
	16. PRICE CODE

17. SECURITY CLASSIFICATION OF REPORT	18. SECURITY CLASSIFICATION OF THIS PAGE	19. SECURITY CLASSIFICATION OF ABSTRACT	20. LIMITATION OF ABSTRACT
UNCLASSIFIED	UNCLASSIFIED	UNCLASSIFIED	UL

EXECUTIVE SUMMARY

Compared to many other forging methods, radial forging is relatively new having been commercialized late in the twentieth century. Radial forging may be characterized as a multi-hammer, open die forging process for producing solid and hollow, rotational and non-rotational, axisymmetric parts. Two types of machines are in common usage employing either two or four hammers. Of the various radial forging machines, Gesellschaft fuer Fertigungstechnik und Maschinenbau GmbH (GFM) is the most widely recognized manufacturer.

This report summarizes the state-of-technology in radial forging. A brief presentation of the computer program, RFORGE, which was developed by Battelle under an earlier contract is included (RFORGE User's Manual is included in Appendix A) as are initial results of a reduced scale, isothermal simulation of the radial forging process using the present preform design. The simulation was run using the computer program DEFORM which was also developed by Battelle specifically for simulating metal forming processes. RFORGE was found to be useful for situations where detailed process analyses are not required. However, RFORGE's lack of post-processing capabilities requires that the user manually process and interpret the results. On the other hand, DEFORM was found to be very useful in modeling the radial forging process and offers the user detailed post-processing and information on strain, strain rate, temperature, and metal flow. To simplify the finite element process model used in this study, the simulation was approximated as an isothermal, axisymmetric process. Simulation results are included.

Data supplied by Benet Laboratory was analyzed using statistical methods to determine what significant relations exist between the forged and heat treated gun tube and resultant mechanical properties. Due to probable confounding effects of the forging and heat treatment processes no significant relations were found. It is recommended that a more detailed experimental study be carried out which isolates the forging process from post-forging heat

treatment in order to gain a better understanding of how the radial forging process affects the mechanical properties of the forged gun tube. A simple true strain method of calculating forging reduction was used to analyze the plastic strains at the breech end to develop a new preform design which is expected to yield uniform amounts of strain at each point in the gun tube after radial forging.

TABLE OF CONTENTS

INTRODUCTION 1
Variables in Radial Forging 5
RADIAL FORGING MACHINES 7
Two Die Radial Forging Machines 7
I. Fenn Manufacturing Radial Forging Machine 7
II. Ruthner Radial Forging Machine 7
Four Die Radial Forging Machines 9
I. Kocks Four Die Swing Forging Machine 9
II. GFM Radial Forging Machine 10
III. SMS Hasenclever Radial Forging Machine 12
Radial Forging Machine Drives 12
Radial Forging Automation 14
Forging Over A Mandrel 15
RADIAL FORGING RESEARCH 18
Metal Flow in Radial Forging 21
Cold and Warm Forging 24
Defect Consolidation 24
USE OF RFORGE PROGRAM 26
FINITE ELEMENT MODELING OF RADIAL FORGING 28
Discussion of Results 30
PRE-FORM DESIGN FOR 155 MM GUN TUBE 36
Preform Design for Desired Product Properties 42
Grain Growth and Recrystallization Kinetics 43
Effect of Deformation Parameters on Recrystallization 44
Effect of Grain Refiners on Recrystallization 45
Preform Development 46
CONCLUSIONS AND FUTURE WORK 54
REFERENCES 55
APPENDIX A: RFORGE USER'S MANUAL 59

LIST OF FIGURES

Figure 1. Radial Forging Process.....2
Figure 2. Open Die Forging Process (Ref. 3).....3
Figure 3. Cross-section of the GFM Radial Forging Machine (Ref. 6).....4
Figure 4. Two Die Radial Forging Machine (Ref. 8).....8
Figure 5. Three Die Radial Forging Machine (Ref. 4).....8
Figure 6. Kocks Swing Forging Machine (Ref. 4).....10
Figure 7. GFM Four Die Radial Forging Machine (Ref. 10).....11
Figure 8. SMS Hasenclever Four Die Radial Forging Machine with Tool and Workpiece Motions (Ref. 11).....13
Figure 9. A Radial Forging Line at Carpenter Technology's Plant (Ref. 13)....15
Figure 10. Deformation Zones in Radial Forging of Tubes (Ref. 15).....17
Figure 11. Deformation Zones in Radial Forging of Solids (Ref. 15).....17
Figure 12. Velocity Field in Radial Forging Showing Effect of Relative Indentation to Core Penetration (Ref. 1).....23
Figure 13. DEFORM FEM Process Model Using Rigid Dies and Axisymmetric Geometry.....32
Figure 14. DEFORM Velocity Field After 0.273 Inches Penetration.....33
Figure 15. DEFORM Mesh After Indexing Workpiece Axially 3.00 Inches.....34
Figure 16. DEFORM Strain Distribution After Indexing and 0.273 Inches Penetration.....35
Figure 17. Yield Strength Plots for AISI 4337 Steel Data.....38
Figure 18. Tensile Strength Plot for AISI 4337 Steel.....39
Figure 19. Charpy Impact Values for AISI 4337 Steel.....40
Figure 20. Experimental Preform Design (Ref. Sketch 7-89).....48
Figure 21. Polar Coordinate Notation.....48
Figure 22. Definition of Geometric Regions.....50
Figure 23. Notation for Calculation of Frustum Volume.....52
Figure 24. New Preform Design for Benet Laboratory.....53

LIST OF SYMBOLS

1. α = Die Half Angle
2. $B = (\tan \alpha + \mu)/\tan \alpha$
3. β = Fraction of Deformation Energy Converted to Heat
4. C = Flow Stress Constant
5. c = Specific Heat
6. D = Mean Tube Diameter
7. D_{gr} = Mean Grain Diameter
8. $\dot{\varepsilon}$ = True Strain Rate
9. ε = True Strain
10. J = Mechanical Equivalent of Heat
11. m_1 = Friction Factor at Tool Surface
12. m_2 = Friction Factor at Mandrel Surface
13. μ = Coulombic Coefficient of Friction
14. n = Strain Rate Exponent
15. P = Radial Die Pressure
16. R_e = Outside Radius at Exit of Deformation Zone
17. R_m = Outside Radius of the Mandrel
18. r_p = Mean Radius of Second Phase Particle
19. R = Outside Radius at a Specified Location
20. ρ = Specific Weight
21. σ_0 = Flow Stress (Tensile)
22. σ_1 = Maximum Principal Stress
23. σ_1^0 = Stress at Zero Reduction
24. σ = Flow Stress in Compression
25. σ_b = Back Push in Swaging
26. σ_e = Flow Stress at Exit of Deformation Zone
27. σ_z = Axial Flow Stress
28. t = Wall Thickness
29. T_D = Temperature Increase due to Deformation
30. v_f = Volume Fraction of Second Phase Particles

Note: A subscript of zero refers to the original dimension or value of the quantity.

INTRODUCTION

Metal forming processes may be divided into two broad classifications depending on their flexibility. Lange has proposed such a scheme where metal forming is divided into free-flow forming and restricted-flow forming processes (Reference 1). According to this definition, the final shape and tolerance of the workpieces in free-flow forming is dependent only on the relative motions and positions of the dies. Restricted-flow forming on the other hand is independent of machine motion and is a function of the die impression only based on Lange's classification. Based on these definitions it is readily seen that radial forging may be broadly classified as a free-flow forming process. Additionally, it is apparent that radial forging is a flexible forming process in that a variety of different part geometries can be produced without any requirements for die change.

Radial forging often referred to as, and confused with, rotary forging is a relatively new forging process. The term rotary forging is used due to the fact that in some operations the workpiece is rotated during the forging operation. The term, radial forging, appears to be widely used in Europe to describe the process while both radial and rotary forging are commonly used in the United States to describe the process. The process is depicted in Figure 1 below.

A similar process that may be classified as a form of radial forging is rotary swaging. Swaging differs from radial forging in that the dies are mounted in a headstock which holds the dies and a set of planetary rollers. Typically, two or four dies are used. The end of the dies which contacts the rollers is shaped as a cam. As the headstock rotates at a high frequency the dies are activated by the rollers and returned by centrifugal force. The die travel is changed by adding or removing shim stock between the dies and rollers.

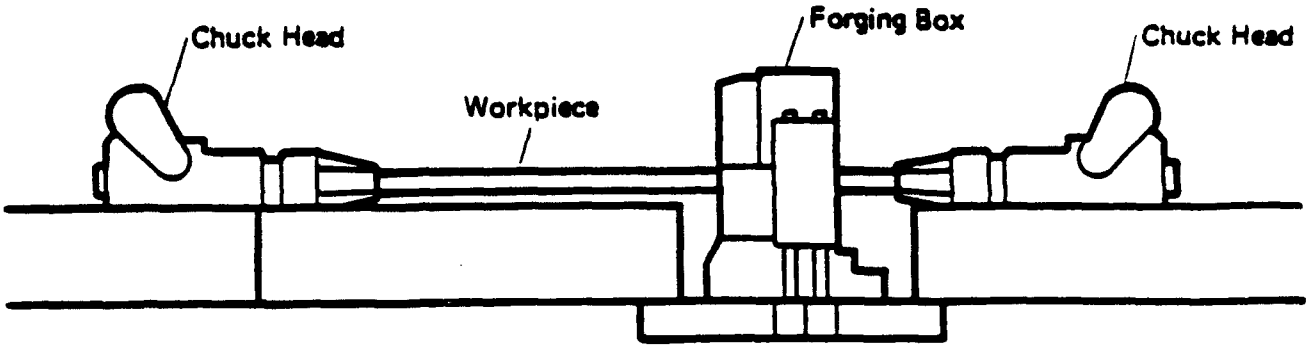

Figure 1. Radial Forging Process.

Radial forging in its present form is essentially an open die forging process using sets of counterblow hammers or dies where tubular (solid or hollow) or square billets are reduced in cross-section to straight or tapered forms. For processing of tubular billets, a mandrel is required. Radial forging is commonly done using 2, 3, or 4 counteracting dies located in one plane. The simplest and most common orientation is the vertical plane. Most forging applications for radial forging involve simple reduction of the cross-section of axisymmetric parts. However, increased use of the process is being made in small lot production of complex "T", "X", and "Y" shapes. Radial forging is also capable in some cases of producing parts of non-symmetric cross-section. However, the machine must be modified to withstand the torque and moment arms developed by the out-of-plane forging conditions (Ref. 2). Additionally, this necessitates that the machine be capable of independent adjustment of the individual hammers.

Rotary forging was developed from open die forging where solid billets are reduced between a flat upper die and a "U" or "V" shaped lower die in a mechanical or hydraulic press. An overhead crane or track mounted manipulator is then used to rotate and feed the billet between subsequent press hits. This process is depicted below in Figure 2:

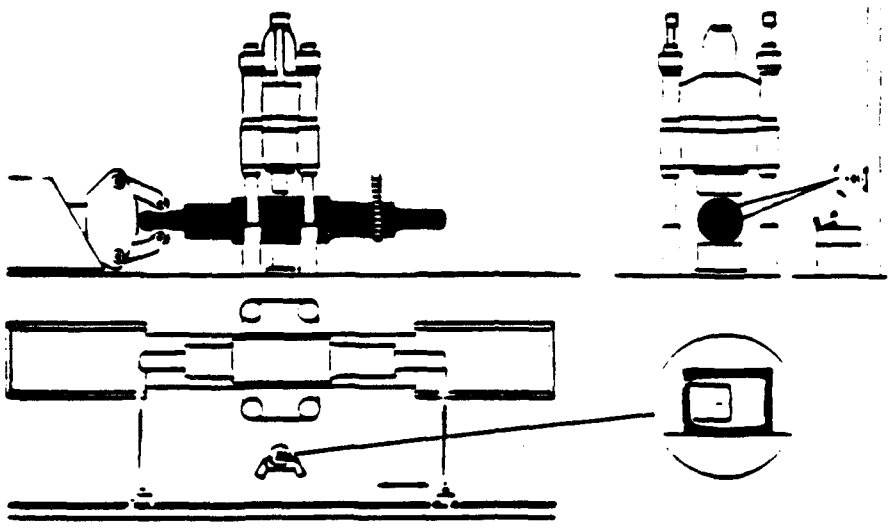

Figure 2. Open Die Forging Process (Ref. 3).

However, there are a number of problems inherent in the open die process depicted in Figure 2. The process is quite slow due to the limitation of stroking rate of the press being used. Due to the die configuration, edge and surface cracks or bursts are likely to develop due to the tensile stresses that can develop in the unsupported edges of the workpiece. Additionally, significant heat loss from the billet to the dies may require that multiple reheats be performed to prevent the material flow stress from becoming too large. Center bursting and surface cracking problems may be minimized by using "V" shaped dies but this limits the amount of reduction available in one pass and may require frequent die changes between passes (Ref. 4). Many of these problems have been overcome by the present radial forging machines.

The basic configuration of the radial forging machine was initially developed by Dr. Bruno Kralowetz who founded GFM in Steyr, Austria in 1946 (Ref. 5). The first four hammer working model of the machine was introduced in 1960. GFM has since installed over 600 machines worldwide. A cross-sectional view of the forging box of a GFM machine is shown below in Figure 3.

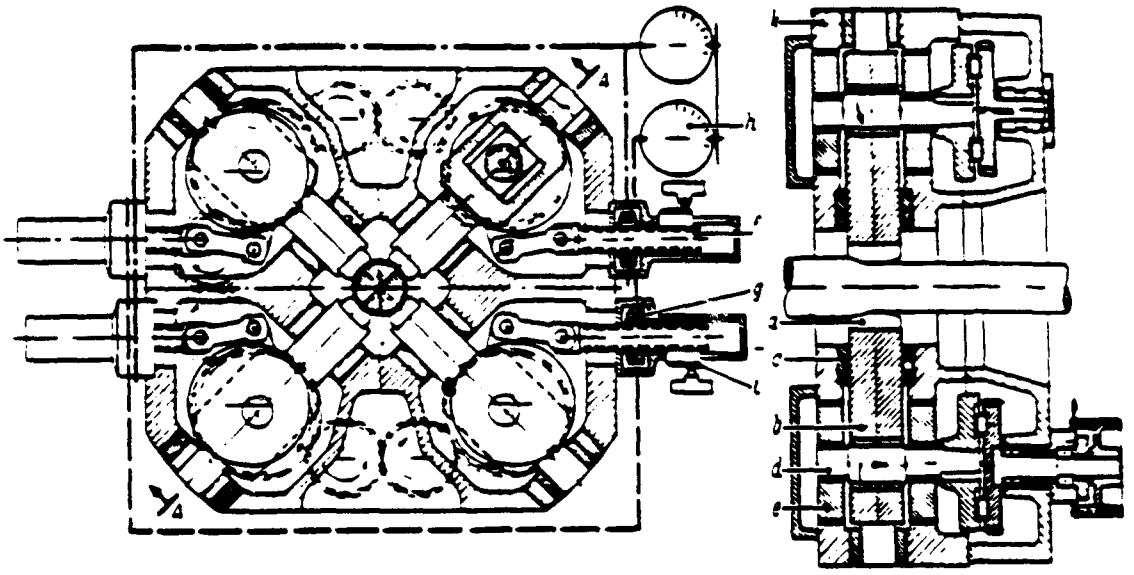

Figure 3. Cross-section of the GFM Radial Forging Machine (Ref. 6).

As can be seen, the basic premise of the machine is that four dies attached to hammers simultaneously press the workpiece. It is important to note the distinction that the dies actually press the workpiece although it would appear that with the high stroking rate that the dies actually act like hammers. However, the deformation rates encountered in radial forging are within those typically encountered for press operations. The radial forging process has a high stroke rate due to the fact that the hammers are spaced very close to the workpiece, requiring only a short period of time between subsequent strokes. As the radial forging machine is simply a short-stroke mechanical press, the die velocity at any point in the stroke may be calculated by using equation (1) below (Ref. 7). Additionally, many machines have an automated stock handling system incorporated into the machine to provide coordinated rotation and feed of the stock between hits. Thus, only a small portion of the workpiece undergoes deformation at a given time. The advantage of using four hammers is that the probability of edge cracks developing from tensile stresses is quite small as the surface is under compression. Due to the counteracting motion of the hammer dies, there are virtually no stresses being transmitted to the forging machine frame and

since only a small portion of the workpiece is being deformed at one time, the forging forces required will be relatively low. Heat loss from the workpiece is minimized and in many cases, with proper selection of process parameters, the temperature may increase from deformation as the hammers contact the workpiece typically from 150-200 times per minute. This is advantageous as it eliminates the need to reheat the billet between passes. The need for die changes are also eliminated with the radial forging machine as the amount of reduction may be varied merely by changing the stroke length of the hammers. On many machines this may be done by simple reprogramming of the machine. Another advantage of the radial forging process is that the internal soundness of cast billets is improved and internal voids closed.

(1) $$V = \frac{\pi NW}{30}\sqrt{\frac{S}{W} - 1}$$ (Ref. 10)

where: W = Ram Location from Bottom Dead Center (inches)
S = Stroke Length (inches)
N = Number of Strokes per Minute

Present day rotary forging equipment is best characterized by the number of hammers used in the machine. Two and four hammer machines being most common. Typical hammer arrangements for each machine are shown below in Figures 4, 5, and 6. Another classification scheme would be to group machines on the basis of whether the hammers are arranged in the vertical or horizontal plane. However, radial forging machines of the latter type are not common.

Variables in Radial Forging

Shown below in Table 1 is a listing of the major variables found in radial forging which must be controlled to obtain desired finish product properties.

Table 1. Significant Variables in Radial Forging Process.

1. Forging Stock or Pre-form Variables:
    - Material Flow Stress
    - Microstructure
    - Stock Dimensions
    - Material Physical Properties (e.g. thermal properties)
    - Scale on Surface of Stock
    - Temperature of Workpiece
2. Machine and Tooling Variables
    - Die Geometry
    - Die Material and Properties
    - Mandrel Properties and Design
    - Use of Lubricant on Mandrel
    - Stroking Rate
    - Length of Stroke
    - Machine Tonnage Capacity
3. Process Variables
    - Billet Temperature
    - Die Stroke Velocity/Contact Time on Workpiece
    - Percent Reduction of Workpiece
    - Temperatures Generated in Work Zone
    - Feed Rates (Axial and Longitudinal)

RADIAL FORGING MACHINES

Two Die Radial Forging Machines

Two die radial forging machines are quite similar to traditional open die forging presses in that two dies are used. Radial forging machines on the other hand have a much higher stroking rate than traditional mechanical presses.

I. Fenn Manufacturing Radial Forging Machine

A schematic of a two hammer radial forging machine built by Fenn Manufacturing Company under license from Usine de Wecker is shown below in Figure 4 (Ref. 8). As of 12/31/89, the manufacture of these machines in Europe was transferred to GFU-Maschinenbau GmBH of West Germany (Ref. 8). With suitable alteration, the machine can also operate with four dies. As can be seen, the dies are mounted on rocker arms driven by a single driveshaft via eccentric cams. The dies are returned by spring action after deforming the workpiece. The distance between the dies is controlled by adjusting a worm type bushing which controls the throw of the dies or chuckheads which also advance the part in the axial direction. Due to the rapid stroking of the dies, significant heat buildup can occur in the dies. To avoid overheating, the dies are water-cooled. As can be seen in Figure 4, the Fenn Machine is a relatively simple mechanism. Maximum operating speed is 1000 strokes per minute with forging loads of 15,000 KN per tool (Ref. 8).

II. Ruthner Radial Forging Machine

The two die hydraulic radial forging machine from the Andritz-Ruthner Industrieanlagen-Akliengeselleschaft of Austria was first introduced in 1981 (Ref. 9). The forging box consists of two horizontally arranged hydraulic cylinders upon which the forging dies are mounted. Some of the machine features include 1,250 tons capability per tool, automatic tool-changing and pre-heating, and a hydrostatic mounting system for the manipulators. The uniqueness of the hydrostatic mounting system stems

from the fact that the base of the manipulators ride entirely upon a layer of oil in order to eliminate all metal to metal contact and wear (Ref. 9).

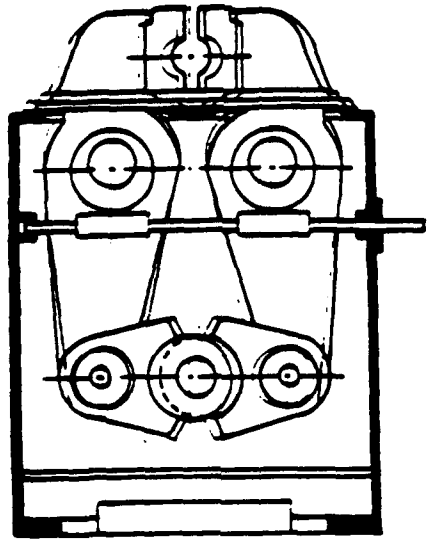

Figure 4. Two Die Radial Forging Machine (Ref. 8).

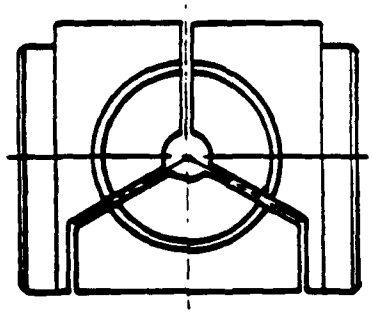

Figure 5. Three Die Radial Forging Machine (Ref. 4).

Due to the two hammer layout of the Ruthner machine, the forging of round stock requires multiple forging passes. Initially the billet is pass forged to achieve an octagon shape slightly larger than the finish forged dimension while the final pass forges the finish dimension using short strokes to obtain small depth penetration at the surface (Ref. 9).

Four Die Radial Forging Machines

In general, the four die radial forging machines are more widely used than two die machines. One of the major advantages of the four die machines is that square and round shapes may be produced in one pass whereas the two die machines often require multiple forging passes. In general, four die machines are more complex and costly than two die machines.

I. Kocks Four Die Swing Forging Machine

This machine differs from other radial forging machines in that the dies are activated by mechanical linkages and eccentric cams as shown in Figure 5. Most four die machines are driven by either hydraulic pistons or mechanical connecting rods. Additionally, the Kocks machine differs from other radial forging machines in that it is intended mainly for hot reduction of square or rectangular billets on a continuous basis, similar to rolling (Ref. 4).

Each die is operated independently by three linkages mounted on eccentric cams. The dies are operated in pairs with the second pair operated at 180 degrees to the first pair. The machine is self-feeding and requires no manipulators to feed the stock as the dies pull the material through the forge zone after deformation. The dies initially sink the material as shown in Figure 6a. With continued travel of the dies, the material is finish forged and pulled through at the end of the die rotation.

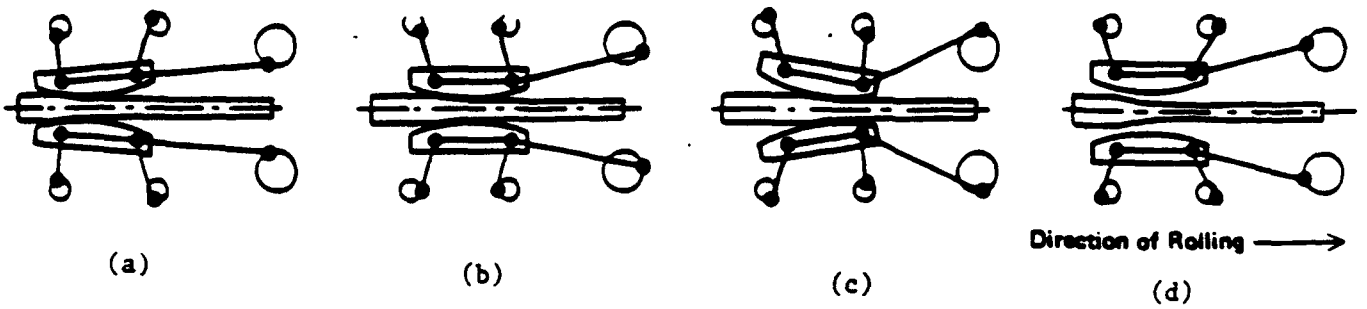

Figure 6. Kocks Swing Forging Machine (Ref. 4).

II. GFM Radial Forging Machine

The four die configuration of the radial forging machine is probably the most common machine in use. Of these, GFM is best known for radial forging machines.

The first radial forging machines built by GFM were based on a pneumatic-hydraulic drive system which closely approximated the action of a counterblow hammer. A schematic of the machine is shown below in Figure 7. The dies were activated by a high pressure nitrogen system connected to individual pistons. This enabled the dies to achieve high impact energies and velocities up to 30 feet/second (Ref. 10). Synchronization was provided by a hydraulic system to maintain die travel. Upon completion of the forming stroke, the dies were retracted by the hydraulic system which also acted to compress the nitrogen gas (Ref. 10). The machine was capable of preheating the stock with the addition of an induction heater mounted at the entrance to the forge box. This system has been replaced in favor of the mechanical drive system described below.

The present four hammer GFM radial forging machine is essentially a mechanically driven short stroke press. Due to the close proximity of the hammers in relation to one another, very high stroking rates are achieved.

This is a major change from the GFM machine described above. Each die is mounted on a connecting rod which is driven by an adjustable eccentric shaft which enables variable stroke lengths. The eccentric shafts are driven via gears which synchronize the amount of die travel. Both round and rectangular cross-sections may be reduced as die travel may be adjusted either in sets or in unison via gears in the forging box. GFM's largest machine used in the West, the SX-65, is capable of 125 strokes per minute with a forging load of 25,000 KN per tool (Ref. 6). A larger model, the SX-85, has been delivered to the Soviet Union.

The construction of the GFM radial forging machine is radically different from that of typical open-die forging presses. The forging action of the radial forge takes place within a vertically arranged forging box which houses the four hammers and drives at right angles. Due to the opposing motion of the hammers, no forces are transmitted to the machine itself. Therefore the machine foundation remains virtually free from stress and vibration (Ref. 6).

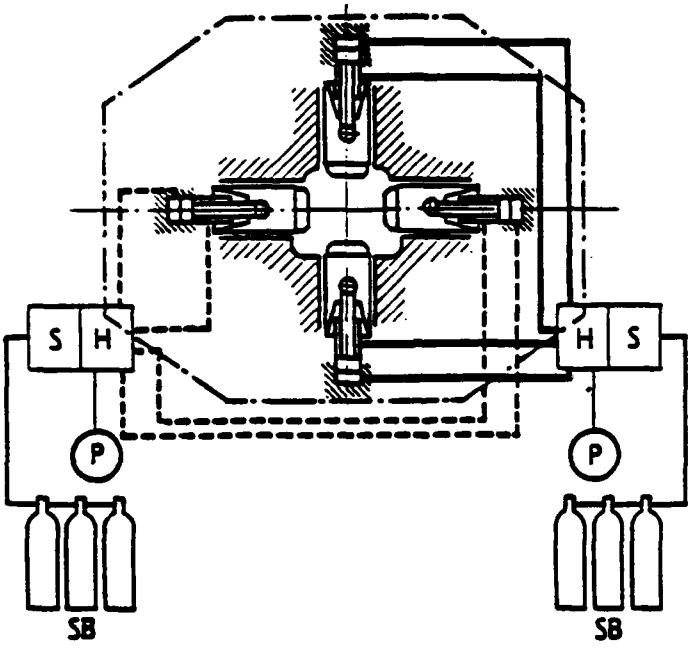

Figure 7. GFM Four Die Radial Forging Machine (Ref. 10).

III. SMS Hasenclever Radial Forging Machine

A rather unique four hammer radial forging machine was developed by SMS Hasenclever in collaboration with the Technical University of Stuttgart to forge tubular and solid billets. A cross-sectional view of the RUMX 2000 is shown below in Figure 8. The uniqueness of the RUMX 2000 derives from the fact that it allows individual control of each ram stroke and adjustment of the stroke length and position between each stroke. Another feature of the RUMX 2000 is a programmable tool change system which enables quick change capability of the dies during the process which allows a workpiece of 550 square mm to be reduced to 65 mm diameter without interruption (Ref. 1). With appropriate modifications, the RUMX 2000 is also capable of forging non-symmetric workpieces.

The hammers are hydraulically driven and have a maximum capacity of 10 MN. Machine control is provided by a DEC PDP 11/73 computer (Ref. 1). The control computer also generates process plans and appropriate processing control program from the finished workpiece geometry using the computer program "PRORUM" as described below.

Radial Forging Machine Drives

A review of the common radial forging machines show that two drives are in common use: mechanical and hydraulic. Of these two, mechanical drives are predominant. The primary reason for the popularity of the mechanical drive is due to the inherently faster speed of the drive compared to a hydraulic system. However hydraulic drives offer greater flexibility in forging prismatic and non-symmetric cross-sections due to the possibility for individual control of each hammer's stroke.

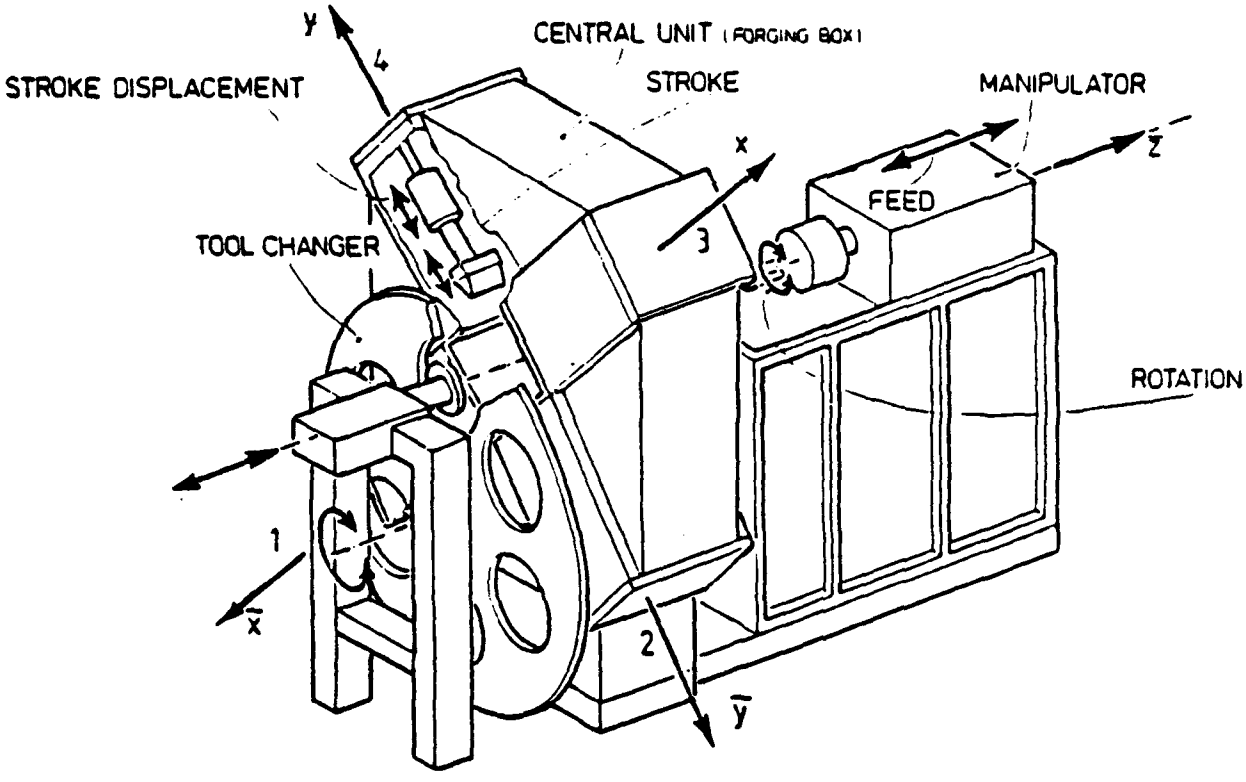

Figure 8. SMS Hasenclever Four Die Radial Forging Machine with Tool and Workpiece Motions (Ref. 11).

Radial Forging Automation

One common feature of most radial forging machines is integral, automatic stock handling by one or two manipulators. For the case where the workpiece must be forged over its entire length in one heat, two chuckheads are normally used (Ref. 12). In the case of two manipulators, one manipulator serves to feed the workpiece while the second manipulator merely holds the workpiece and maintains centering. The stock manipulators serve to provide both longitudinal and rotational movement to the workpiece. Workpiece movement occurs between hammer blows to prevent twisting of the workpiece. Unlike open die forging, the manipulators constantly maintain the workpiece center position between the dies irregardless of the cross-section reduction. The manipulators perform both axial and rotational feed between strokes.

Many radial forging installations have completely automated processes integrated into flexible manufacturing systems (FMS). A typical example of an automated radial forging operation is the line at Carpenter Technology's forge plant in Reading, PA which was installed in 1983. This line is depicted in Figure 9 below. Another example of an automated radial forging line that integrates forging, heat treatment, and automatic stock handling operations, is located at the U.S. Army's Watervliet Arsenal in Watervliet, NY.

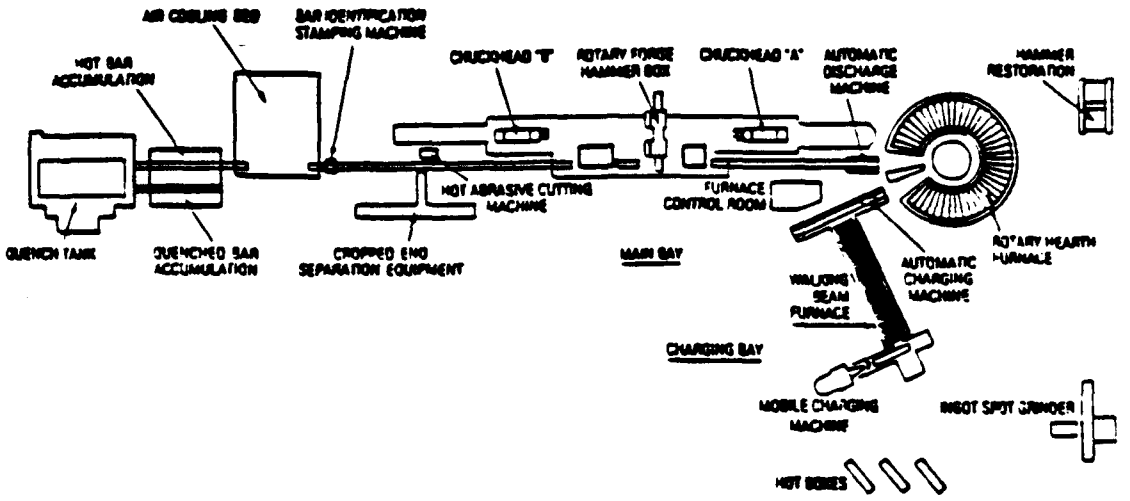

Figure 9. A Radial Forging Line at Carpenter Technology's Plant (Ref. 13).

Forging Over A Mandrel

The primary difference between forging solid and hollow workpieces is that a mandrel must be used. For hot and cold forging of seamless tubes in radial forging, a retractable mandrel must be employed to support the inner wall of the workpiece. An additional difference is that three deformation zones exist during tube forging whereas solid forging has only two deformation zones. This is depicted below in Figures 10 and 11. Typically the mandrel is a hardened piece of tool steel with internal water cooling to prevent seizure due to exposure to the high temperatures and pressures generated during the forging process. The outer diameter of the mandrel corresponds to the finished inner diameter of the forged workpiece. Two types of mandrels are commonly used in radial forging. The first is a "short" or stationary mandrel which is used to forge tubes having a constant internal bore (Ref. 12). The second type is termed a "long" or moveable mandrel and is used to forge tubes having stepped inner and outer diameters (Ref. 12). The long mandrel moves in progression with the workpiece through the deformation zone while the short mandrel remains stationary. Due to the fine surface finishes from cold forging, some work has been done in finish

forging the rifling in small caliber, thin wall gun barrels (Ref. 14). Due to the presence of high temperatures and pressures at the mandrel/workpiece interface, in many cases adequate lubrication or an insulating material may need to be applied to the mandrel to prevent sticking.

The stresses on the mandrel were analyzed by Ragupathi et al. (Ref. 16) using the computer program, ADINA, which is based on the finite element method. An examination of the stresses on the mandrel show that it subjected to both thermal and mechanical stresses. Thermal stresses are set-up due to the creation of large thermal gradients between the water-cooled mandrel and the heated workpiece. Mechanical stresses arise due to the intermittent loading from the hammers. Ragupathi et al. (Ref. 16) reported that the thermal stresses remained relatively constant during the process due to the constant nature of the temperature gradients whereas the mechanical stresses could be modeled using a sinusoidal waveform. Since the dies operate at 200 strokes/minute, both the dies and mandrel are subject to fatigue failure (Ref. 17).

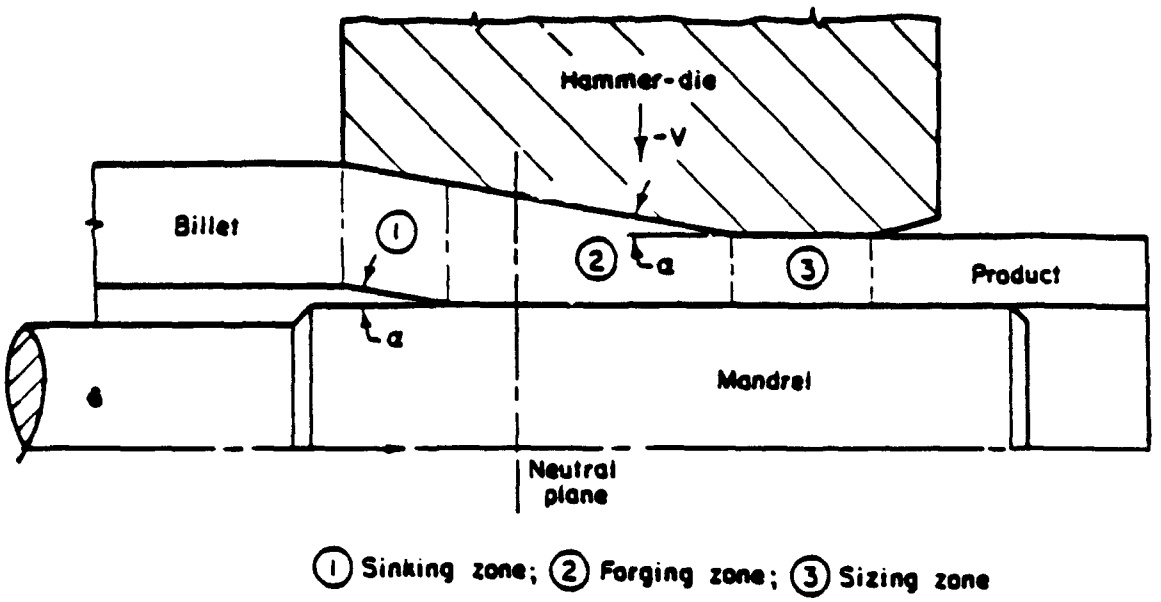

Figure 10. Deformation Zones in Radial Forging of Tubes (Ref. 15).

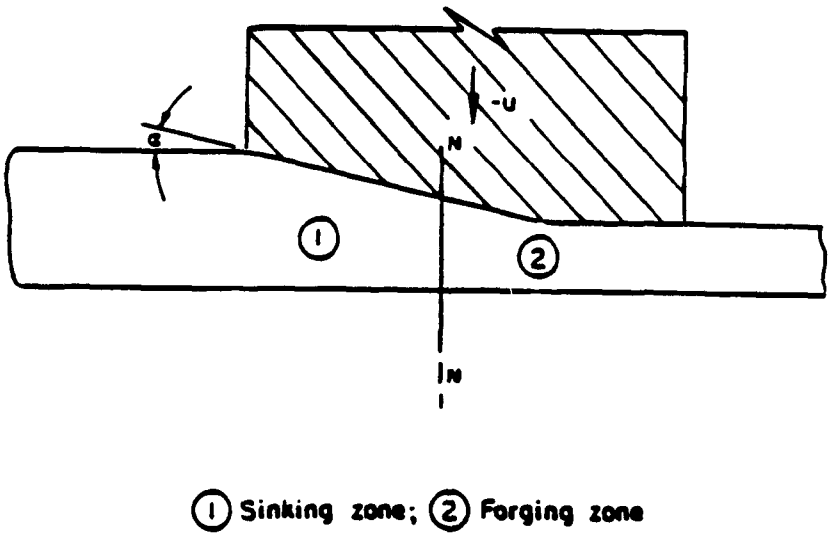

Figure 11. Deformation Zones in Radial Forging of Solids (Ref. 15).

RADIAL FORGING RESEARCH

The first significant paper was written by Sachs and Baldwin in 1946 where they analyzed the stress states in tube drawing (Ref. 18). While tube sinking is not a radial forging process per se, it is quite relevant in that the material deformation and stress states are similar to those in tube sinking in radial forging. Sachs and Baldwin were the first to apply the slab approach to analyzing the tube sinking process. The resulting expression for the draw stress is shown below in equation (2).

$$(2) \qquad \sigma_1 = \frac{Bk_0}{B-1}\left[1-\left(\frac{D}{D_0}\right)^{B-1}\right]+\sigma_1^0\left(\frac{D}{D_0}\right)^{B-1}$$

Their result shows that the draw stress is a function of the tube reduction and the existing friction conditions at the workpiece and die interface.

The next noteworthy paper was presented by Kegg in 1964 on the mechanics of rotary tube swaging (Ref. 19). Kegg attempted to develop a model for the kinematics of the headstock mechanism and for predicting the power requirements for the process and estimating the maximum reduction. The model that Kegg used in his analysis for determining the die pressure assumed that the radial forging process was similar to plane strain extrusion with a small inlet angle. The resulting equation from the slab analysis shows that the die pressure is a function of the back push stress material flow stress and the deformation, x.

$$(3) \qquad \sigma_1 = \left(\sigma_b + \frac{2}{\sqrt{3}}\sigma_0\right)\exp\left(\frac{2\mu x}{h}\right)$$

Examining equation (3) above it can be seen that the result is very similar to the case for extrusion. However, this analysis ignores the effect of the finishing zone which has been shown to be a significant effect in radial

forging (Ref. 15). Additionally, the assumption that the die inlet angle, α, is small is not always valid in radial forging practice.

No further work was done in this area until 1974 when researchers at Battelle Columbus Laboratories analyzed the radial forging process for manufacturing gun barrels for the United States Army (Ref. 15). This effort was the first to extensively mathematically model the radial forging process. As part of the work, slab and upper bound analysis of the forging of gun tubes was performed to predict the stresses, strains, and temperatures during the forging process. The resultant work was incorporated into a FORTRAN based computer program called RFORGE which enabled calculation of the neutral plane, forging loads, strain, strain rates, and temperatures generated in the workpiece during the forging operation. RFORGE is limited, however, to the forging of tubular workpieces.

The analysis carried out by Altan et al. (Ref. 15) assumed that the radial forging process was divided into three distinct zones: sinking, forging, and sizing. Additionally, complete contact around the periphery was assumed between the dies and workpiece such that no flash was generated. An important departure from previous analyses was that the coefficient of friction was replaced by the friction factor. Use of the friction factor enables determination of the friction conditions existing in metal forming by the use of the relatively simple ring test. Additionally, the ring test was used to generate the flow curves for the work material at warm and hot working temperatures.

The resultant equations obtained for the sinking zone from the slab analysis were found to be for the axial stress and die pressures respectively (Ref. 15):

$$(4) \qquad \sigma_1 = \sigma_e - \bar{\sigma}\left\{\left(1+\frac{m_1}{2\sqrt{3}\tan\alpha}\right)\ln\left(\frac{R-0.5t_0\cos\alpha}{R_e-0.5t_0\cos\alpha}\right)+\frac{m_1}{\sqrt{3}t_0\sin\alpha}(R-R_e)\right\}$$

(5) $$P = \frac{t_0}{R}(\bar{\sigma} - \sigma_1)(\cos\alpha)^2$$

The resultant equations for axial and die pressures in the forging zone were found to be respectively (Ref. 15):

(6) $$\sigma_z = \sigma_{ze} - \left[\left(1 + \frac{m_1(1+\tan^2\alpha)}{\tan^2\alpha}\right)\ln\left(\frac{R^2 - R_m^2}{R_e^2 - R_m^2}\right) + \frac{m_2}{\sqrt{3}\tan\alpha}\ln\left[\frac{(R_e + R_m)(R - R_m)}{(R_e - R_m)(R + R_m)}\right]\right]$$

(7) $$P = \bar{\sigma} - \sigma_z$$

The resultant equations for the axial and die pressures in the sizing zone were found respectively to be (Ref. 15):

(8) $$\sigma_z = \sigma_{ze} + \frac{2}{\sqrt{3}}\bar{\sigma}\left[\frac{m_1 R_2 + m_2 R_m}{(R_2 + R_m)t_1}(z - z_e)\right]$$

(9) $$P = \bar{\sigma} - \sigma_z$$

Lange developed a computer program for optimizing the radial forging process for the four hammer hydraulic machine, RUMX 2000, designed at the University of Stuttgart and SMS Hasenclever (Ref. 1). The program was called "PRORUM" and using the geometry of the final machined part, strains, machining allowance, available raw material dimensions, and available tool sets, the inputs for an automated process planning were generated. PRORUM was a significant breakthrough in the application of NC to metal forming in that all necessary forming steps in the part program were generated from the input data. From the above data, PRORUM adapted the geometry to the radial forging process, determined a suitable preform size, and optimum deformation sequence. In the next phase of the program, the individual process steps are determined including axial and angular feeds, ram motions, and which of the available tool sets should be used to obtain the desired degree of plastification of the cross-section. The program is of an interactive nature and is capable of displaying the workpiece at various intermediate

steps. Additionally PRORUM determines if there is any danger of tool collision based on the tool sets chosen for the process.

Lange further extended the program PRORUM to cover optimization of stepped shaft production for radial forging and turning combined into a complex FMS cell (Ref. 20). The program, "VORUM" was similar to PRORUM in that it was specifically written for the SMS Hasenclever RUMX 2000 Forging machine. VORUM, a multi-function program, is able to select the processing steps for a complex FMS cell which allows optimum use of both the radial forging machine and the lathe to produce a given stepped shaft. Based on the overhead and production costs input as data to the program, VORUM determines all possible process combinations based on a breakdown of the part geometry and then selects the sequence of forging and/or turning that offers minimum processing time and production costs.

The disadvantages of the programs PRORUM and VORUM are that they are proprietary and were specifically developed for the RUMX 2000 machine and are not applicable to general purpose radial forging applications on other forging machines.

Metal Flow in Radial Forging

The metal flow of solid billets in radial forging has been analyzed by Lange (Ref. 1) and Paukert (Ref. 21) at The University of Stuttgart using FEM techniques. Lange's results show that the metal flow is essentially that the material underneath the forming tools will be displaced as a rigid block into the workpiece while the regions to the left and right of the tool will be displaced respectively in those directions with no corresponding plastic deformation. As can be seen below in Figure 12, there is a region where no axial flow of material occurs. This is referred to as the neutral plane. Lange also analyzed the conditions which allowed maximum plastic deformation in a rectangular cross-section using flat tools (Ref. 1). To obtain maximum deformation in the center of the workpiece, described as the ratio of real strain to theoretical strain, Lange found that this occurred when the ratio of

indentation to original billet diameter (bite ratio) was equal to 0.5. To ensure sufficient deformation in the workpiece center, a relative indentation, defined as the ratio of $2^{*}\Delta h/H_{O}$, of at least 0.16 was required (Ref. 1).

Paukert also analyzed the radial forging process using visioplasticity and FEM for a flat forging tool (Ref. 21). Results showed that the most important parameters in radial forging were: ratio of tool length to workpiece thickness, workpiece and tool geometry, and forging sequence. This analysis needs to be extended to the case of tools with compound angles.

Isogawa, Suzuki, and Uehara more recently investigated the radial forging of Inconel 718 in an effort to study the nature of the temperature profile generated and the resultant microstructure (Ref. 22). As part of their study, plasticine was used to model the workpiece. One of the most interesting points brought out during the study was that circumferential cracking occurred in the workpiece at a critical temperature. Unfortunately the authors did not report at which temperature this phenomena was observed.

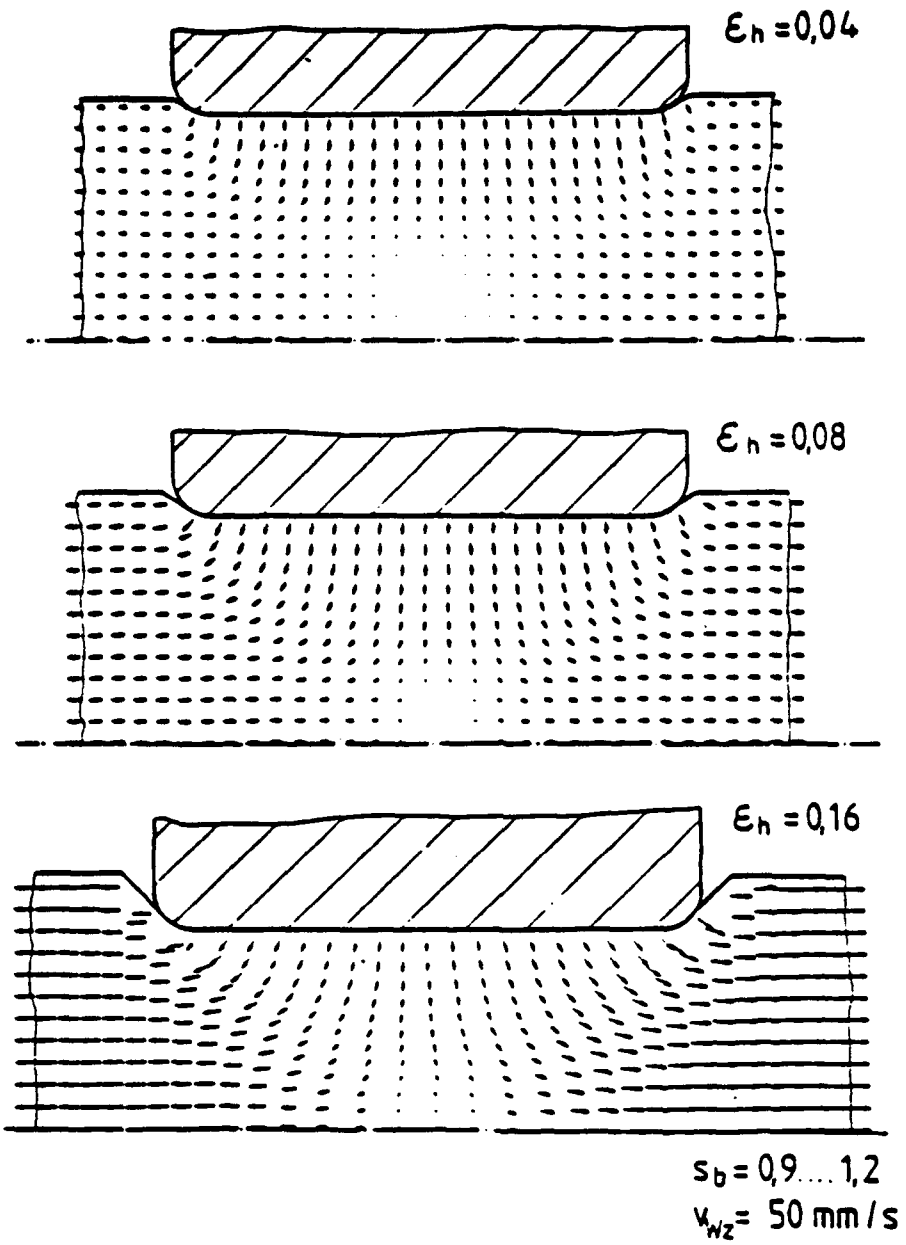

Figure 12. Velocity Field in Radial Forging Showing Effect of Relative Indentation to Core Penetration (Ref. 1).

Isogawa et al. also reported that the shear strain increased from the surface to a maximum value which was located 30% below the surface of the billet. After reaching a maximum, the shear strain rapidly dropped to a negligible amount with increasing distance from the workpiece surface. This corresponded to the region at which the authors reported that circumferential cracking had occurred during actual forging trials. The cracking effect was attributed to the radial and longitudinal tensile stresses that developed in the areas that were between those in contact with the hammers.

Cold and Warm Forging

As the trend towards net shape manufacturing continues, cold and warm forging processes offer several important advantages: reduced energy consumption for billet heating, improved surface finish, and reduced scale formation. The disadvantage is that more robust forging machines are required due to the higher flow stresses encountered. The primary use of cold forging in radial forging is limited to small part production and thin wall tubes due to the higher stresses generated during deformation.

Defect Consolidation

This issue is of considerable importance in the production of wrought billets from cast ingots in primary working processes. Defects are formed from uneven solidification and shrinkage in the casting. These defects seriously impair the soundness and mechanical properties of the final forged product. A large number of studies have been performed to study defect consolidation in open die forging and have been reviewed in an earlier ERC/NSM report (Ref. 23). However this issue has not been studied as extensively for the radial forging process. It would be of practical value to determine how the mechanism of void closure is affected by four radial dies as compared to two dies. Moreover this knowledge would be of use in optimizing the amount of deformation required to close voids which are present in the billet. Closing of voids in open die forging was studied by Im and Dudra (Ref. 23) using both

numerical simulation and plasticine modeling techniques for plane strain conditions in open die forging of massive workpieces. If the assumption that the effect of hydrostatic stress and effective strain are significant as claimed by Im and Dudra, their approach could easily be extended to radial forging. Due to the fact that four hammers are being used rather than two, the internal distribution of compressive stresses should be larger and hence more effective in closing internal voids and porosity. Although this is intuitively obvious, it has not yet been formally studied.

Empirical results from industry have shown that a reduction of 2.2:1 will consolidate centerline porosity to an extent that it can no longer be detected by ultrasonic inspection in wrought bars (Ref. 24). An increase of the reduction to 3:1 has been found to achieve absolute core density and a fine grained structure.

USE OF RFORGE PROGRAM

As part of the first phase of this work, RFORGE computer program was used to simulate the radial forging of gun tubes at The Watervliet Arsenal. RFORGE is presently running on the VAX 11/750 mini-computer at the ERC for Net Shape Manufacturing at The Ohio State University. A user's manual is included in Appendix A, hence only an overview of the program use and capabilities will be presented here.

Three program files: INPUT.DAT, OUTPUT.DAT, and RFORGE.FOR, are required to run the simulation routine. All input, execution and process related variables used in the simulation are entered into INPUT.DAT and are used in the process calculation routines contained in the FORTRAN 77 source file: RFORGE.FOR. Upon completion of program execution, all simulation results are written to and may be accessed from the data file: OUTPUT.DAT. The amount and detail of the output may be controlled by inserting the appropriate variable value in the input data file.

RFORGE is essentially a fixed configuration FEM model for forging of hollow tubes. In its present configuration, RFORGE is limited to simulating forging of AISI 4337 tubular workpieces over a mandrel except in the case where the only item of interest is the forging stresses and loads for which solid, round workpieces may be used. To perform the simulation, the user defines a simplified grid pattern for the workpiece which determines the element sizes after deformation is completed. Deformation is assumed to take place at the end of the stroke. As no plastic deformation is taking place in the sinking zone, only the forging and sizing zones are considered during the analysis. Workpiece temperatures are calculated by determining the amount of deformation under the dies assuming no heat transfer is taking place at that instant. After deformation is completed, heat transfer is then assumed to take place and the resultant temperature for each element is computed. Stress and load calculations are performed using the slab method. The location of the neutral plane is calculated by numerically searching each of the three regions for the point in the velocity field where the material has zero

longitudinal velocity. Additionally, this region also corresponds to the maximum radial pressure.

The RFORGE analysis of radial forging is similar to that of extrusion. However several important differences exist between the physical processes and must be taken into account when using the output from RFORGE. As mentioned earlier, RFORGE calculates the heat added to the workpiece as it occurred at the end of the stroke. In reality the billet is deformed to its final shape in a series of increments during which heat generation and transfer are taking place. As such the heat calculations and transfer gradients in the billet will not be equal for each approach. RFORGE in this case would be an upper bound method which would present a higher temperature distribution than is actually present.

FINITE ELEMENT MODELING OF RADIAL FORGING

At the present time there are two computer programs available at the ERC/NSM which may be used to analyze the radial forging process. The first program is a dedicated computer program, RFORGE, which was developed at Battelle Columbus Labs under contract with Watervliet Arsenal. The second program is the general purpose, FEM based, metal forming simulation package, DEFORM, which was also developed at Battelle.

For the following simulations, the FEM package, DEFORM, was chosen over RFORGE. The reasons for selecting DEFORM were:

1. Greater flexibility and accuracy to model a wide range of process conditions.
2. Ability to account for heat loss effects not directly related to the plastic deformation process.
3. Capability of modeling hollow or solid workpieces.
4. Superior post-processing and graphical display of simulation results.

Initially the radial forging process will be modeled as an isothermal process in order to gain increased experience in the use of DEFORM for modeling the radial forging process. The isothermal assumption is valid due to the fact that in the forging zone that heat lost to the environment is replaced by the heat generated from the dies impacting the workpiece rapidly. The workpiece temperature may in fact be controlled during the process by varying the feed of the workpiece (Ref. 12). However, the isothermal assumption may not be entirely true as the workpiece temperature may actually increase, and hence lower the flow stress, if the processing conditions are favorable. However, radial forging of gun steel is normally done in the hot regime where moderate increases in temperature are not expected to significantly impact material flow stress except in the forging of titanium and nickel based alloys.

Later in the project, the process will be modeled non-isothermally to include the effect of heat loss incurred during transport of the billet before and during the deformation process to study the effects on the material flow stress. Additionally, a more realistic velocity profile will be incorporated to account for the characteristics of die travel similar to that for a mechanical press. As the software becomes available, it is also planned to model the process using three-dimensional FEM.

The results presented in this report consist of two-dimensional, axisymmetric, isothermal simulations for AISI 4337 steel using concave dies. Axisymmetry in the model implies that metal flow was restricted to the axial and radial directions. Use of an axisymmetric model minimized the modeling complexity and simulation time. Inherent in the axisymmetric assumption is that the dies completely encircled the outer surface of the workpiece during deformation. As such, no flash was extruded between the dies in the model. Additionally, this assumption eliminated the need to consider the workpiece rotation between strokes and only the axial feed was considered. To accurately model the process using flat dies, a plane strain model or three dimensional model would need to be developed incorporating the workpiece rotation. Some intermediate and final results of the axisymmetric simulation are shown below in Figures 13-16. The process conditions used in the simulation are shown below in Table 2.

Table 2. Process Conditions Used During DEFORM Simulation.

Die Velocity:	6.299 in/sec. (constant)
Feed Rate:	3.0 inches
Material:	AISI 4337
Billet Temperature:	1652.0 degrees F (900 degrees C)
Heat Transfer:	Isothermal
Stroke Increment:	0.415 inches
Friction Factor:	0.6 (Constant)

Discussion of Results

In Figure 13 the initial mesh and the rigid die used throughout this simulation is shown. The mesh was created using the Automatic Mesh Generator (AMG) and system mesh optimizer packages in DEFORM which automatically configures an optimum mesh based on the workpiece dimensions. For this simulation a 22 x 4 node mesh was generated. To simulate an axisymmetric workpiece, the symmetry axis was oriented along the Y-axis in DEFORM. This enabled the simulation time to be optimized as only the minimum number of elements are included in the mesh eliminating redundant computations. For simplicity, a flat die was used in the simulation. Boundary conditions imposed on the workpiece included no metal flow across the centerline of the billet due to the axisymmetric assumption and no metal flow in the axial direction across the undeformed end of the billet. The latter restriction was based on the assumption that in practice that the 'A' chuckhead would be gripping the workpiece end which will prevent metal flow at the end of the workpiece.

In Figure 14 the deformed mesh is shown with the corresponding flow lines generated by DEFORM. The neutral plane is clearly evident in the center of the plastically deformed region. Examining the flow lines at the neutral plane show that all metal flow is directed to the centerline of the workpiece. Additionally on either side of the neutral plane the flow lines show that metal flow is initially directed downward and then flows in the axial direction as expected for an incompressible material. This result is very close

to the results obtained by Paukert (Ref. 21) shown in Figure 12. Also noticeable is the effect of the friction factor between the tool and workpiece surface. It may be seen that due to the friction conditions specified, some barreling has occurred.

In Figure 15 the rigid die was moved upwards by 3.0 inches to simulate the axial feed of the workpiece. Although it is realized that in practice the feed is less than 3.0 inches, for the simulation it was felt that a smaller feed would not yield as good resolution as a larger feed on the final plots. To perform this second simulation, the deformed mesh from Figure 14 and duplicate deformation and boundary conditions were imposed.

Figure 16 shows the effective strain contours which resulted from the second run. The contours indicate that the material directly underneath the die was displaced downward as a rigid block of material causing adjoining material to be displaced axially. The highest strains were found in the region lying midway between the die and the workpiece centerline. This region was also found by Isogawa et al. (Ref. 22) to be the region where they observed maximum shear strains and circumferential cracking in their study of radial forging of Inconel 718. At the areas directly under the die and at the centerline, the strains were found to be approximately 50 percent of the maximum effective strain values demonstrating that deformation was to the core. An interesting result is shown slightly above the die impression where a wavefront pattern of strains were created along the cross-section due to the restricted metal flow across the undeformed workpiece edge.

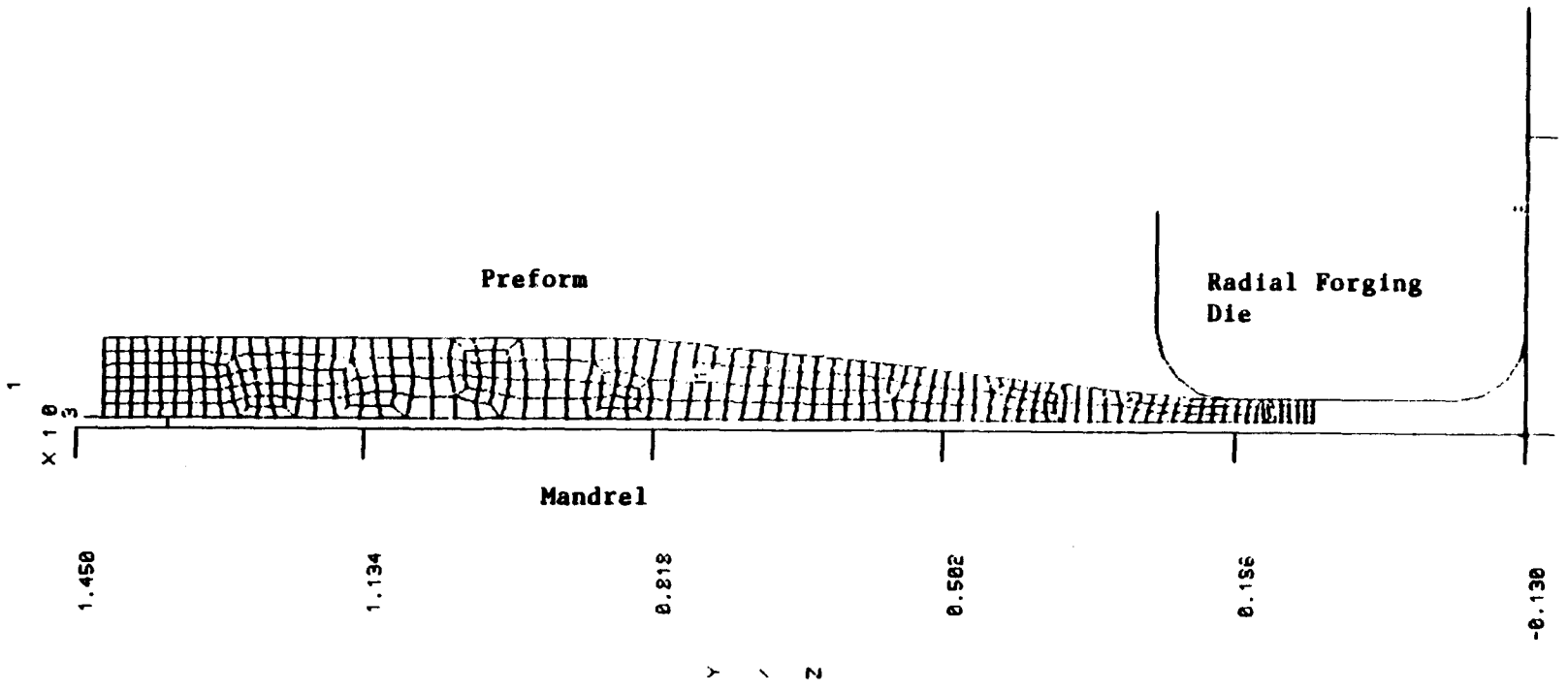

Figure 13. DEFORM FEM Process Model Using Rigid Dies and Axisymmetric Geometry.

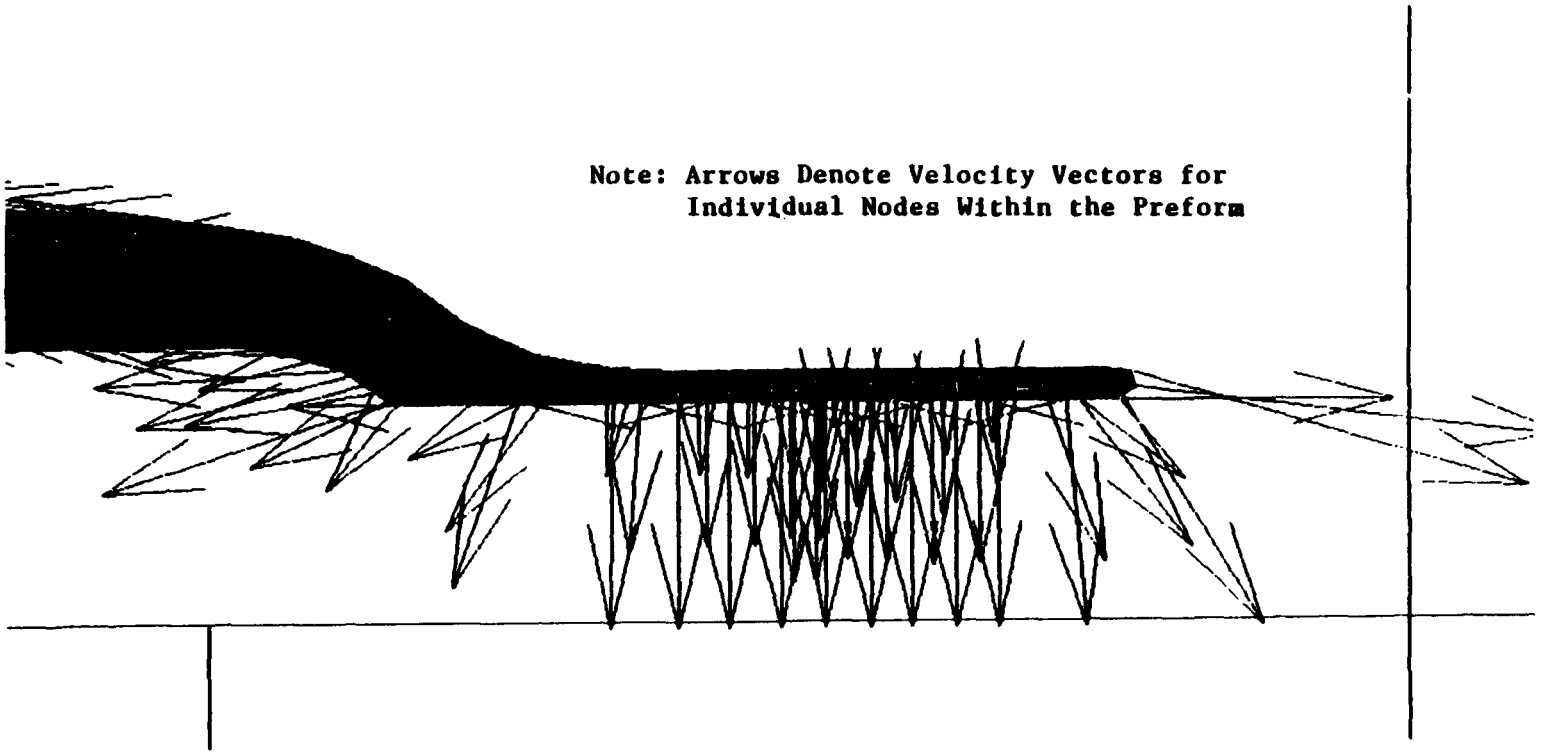

Figure 14. DEFORM Velocity Field After 0.273 Inches Penetration.

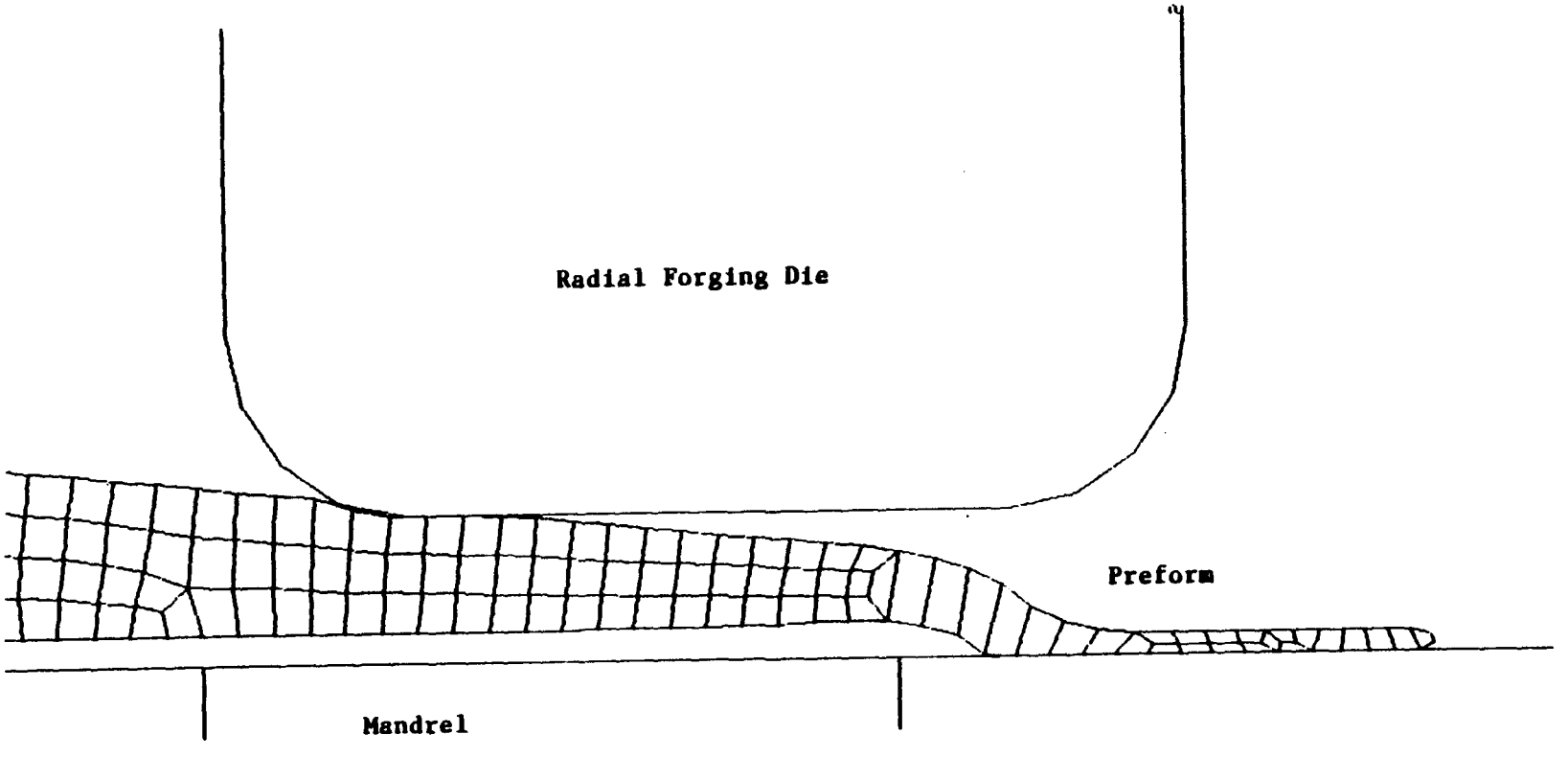

Figure 15. DEFORM Mesh After Indexing Workpiece Axially 3.00 Inches.

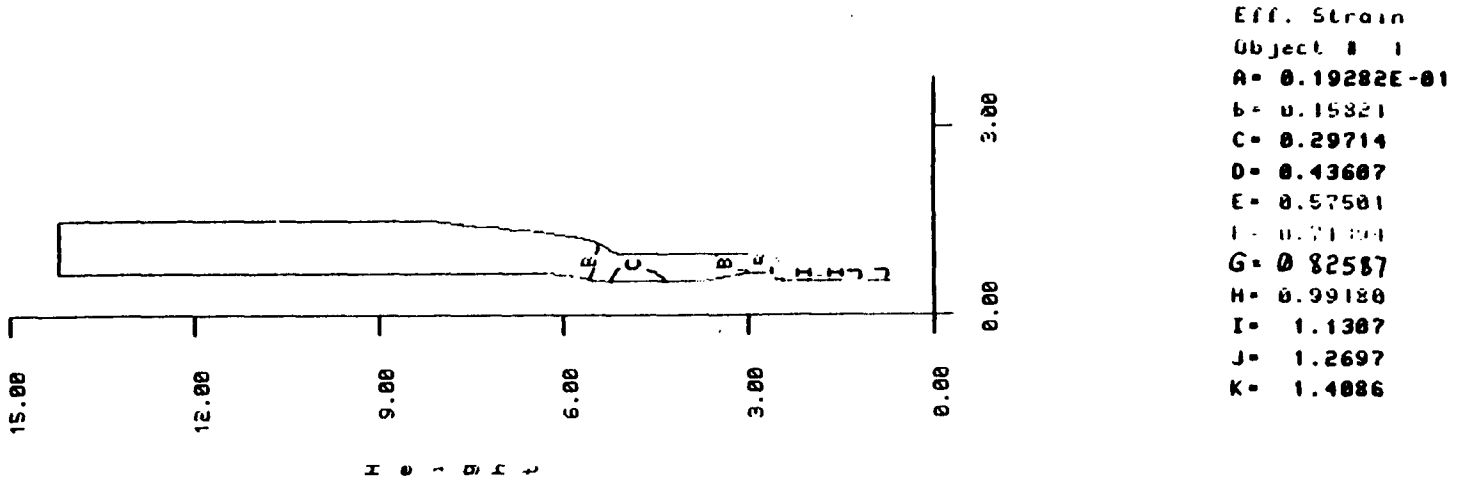

Figure 16. DEFORM Strain Distribution After Indexing and 0.273 Inches Penetration.

PRE-FORM DESIGN FOR 155 MM GUN TUBE

One problem which is of considerable interest in radial forging is designing preforms which will yield a forged product which is near net-shape and/or has consistent mechanical properties. The purpose of this section is to study the experimental data which was provided to the ERC at Ohio State University to analyze for significant factors and to identify an optimum preform for the 155 mm gun tube based on uniform deformation or strain.

The focus of this project resulted from a study at Benet Laboratory which evaluated the mechanical properties of the 155 mm gun tube for consistency after forging and heat treatment. The properties considered in the evaluation were: yield strength, tensile strength, percent reduction of area, percent elongation and Charpy impact values. The data values were taken from a study conducted at Watervliet Arsenal and are shown below in Table 3.

Table 3. Experimental Data From 155 mm Gun Tube Forging.

Total Reduction	Forging Reduction	Yield Strength (ksi) 12, 6 o'clock	Tensile Strength (ksi) 12, 6 o'clock	Charpy Impact (ft.-lbs.) 3, 9 o'clock
4.24:1	1:1	167.1, 164.4	184.8, 183.0	24.0, 23.0
6.39:1	1.5:1	164.4, 162.9	183.0, 179.7	21.0, 24.0
8.55:1	2:1	165.6, 165.6	183.0, 183.0	23.0, 22.0
10.73:1	2.5:1	165.3, 165.0	183.0, 182.4	23.0, 22.0
12.91:1	3:1	165.0, 164.4	182.4, 181.8	22.0, 22.0
15.10:1	3.5:1	165.0, 164.1	182.7, 181.5	22.0, 22.0
17.31:1	4:1	164.4, 164.1	181.2, 181.2	21.0, 23.0
19.52:1	4.5:1	163.2, 163.2	181.5, 181.2	20.0, 21.0
21.75:1	5:1	164.4, 164.4	182.4, 182.4	19.0, 20.0

The most critical factors as identified by Engineers at Benet Laboratory were: yield strength, tensile strength, and Charpy Impact Values. Plots of these data are shown below in Figures 17, 18, and 19. Examining Figures 17, 18, and 19 shows that each of the mechanical properties display small amounts of scatter when plotted against forging reduction. It is also apparent that a trend exists between the mechanical properties and forging reduction. To study the exact relationship and nature of the trend would require taking additional data points. From Table 3 the range of the data was found to be 3.9 ksi, 3.6 ksi, and 5.0 ft.-lbs. for the yield strength, tensile strength and Charpy Impact respectively.

To determine whether the mechanical properties in Table 3 are affected to a significant extent by forging reduction and heat treatment, it was decided to test the data using Analysis of Variance Techniques (referred to as ANOVA). ANOVA methods are powerful statistical methods and procedures used to analyze experimental data (Ref. 26). For the ANOVA analysis presented, a single factor was tested to determine whether or not it was affected by forging reduction and heat treatment or if the variation was due to inherent randomness in the data. Additionally, the difference in location was not considered as a variable but rather as a replication. The specific ANOVA method employed was the single factor ANOVA test. Essentially, the single factor ANOVA is testing two different hypotheses using the well known F-Test to determine whether or not there are differences in the true averages of the different populations due to the treatment (Ref. 26). As the relevant theory and equations are presented in many statistical texts, only the final calculated results will be presented here. The resulting ANOVA tables are shown below in Tables 4, 5, and 6. For the F-test, a significance level of 0.05 was used with eight degrees of freedom (referred to as d.o.f.) for the numerator and nine d.o.f. for the denominator. The critical value, F(0.05,8,9), obtained from a table of F-test values, for rejecting the null hypothesis was 3.23 for all three tests. The null hypothesis for the experiment states that: the

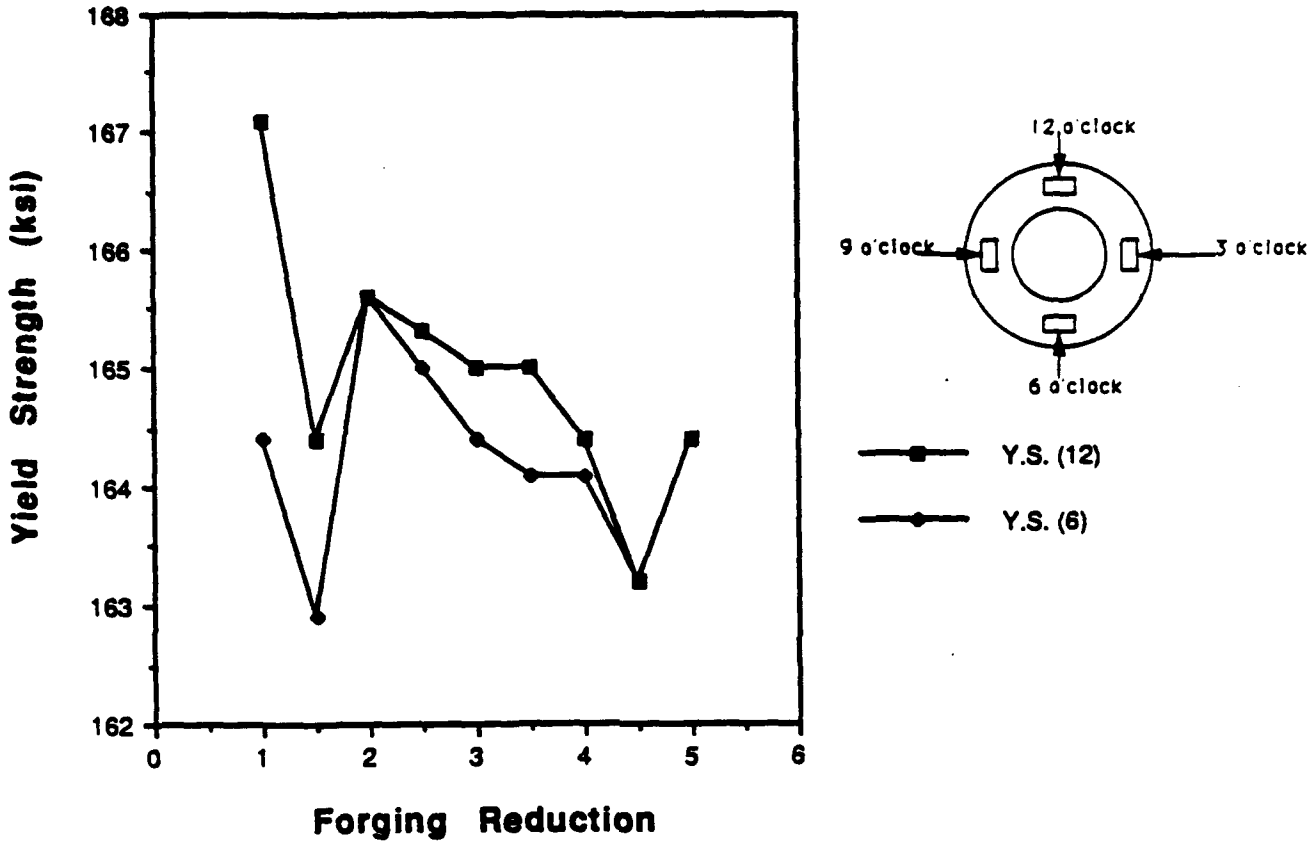

Figure 17. Yield Strength Plots for AISI 4337 Steel Data.

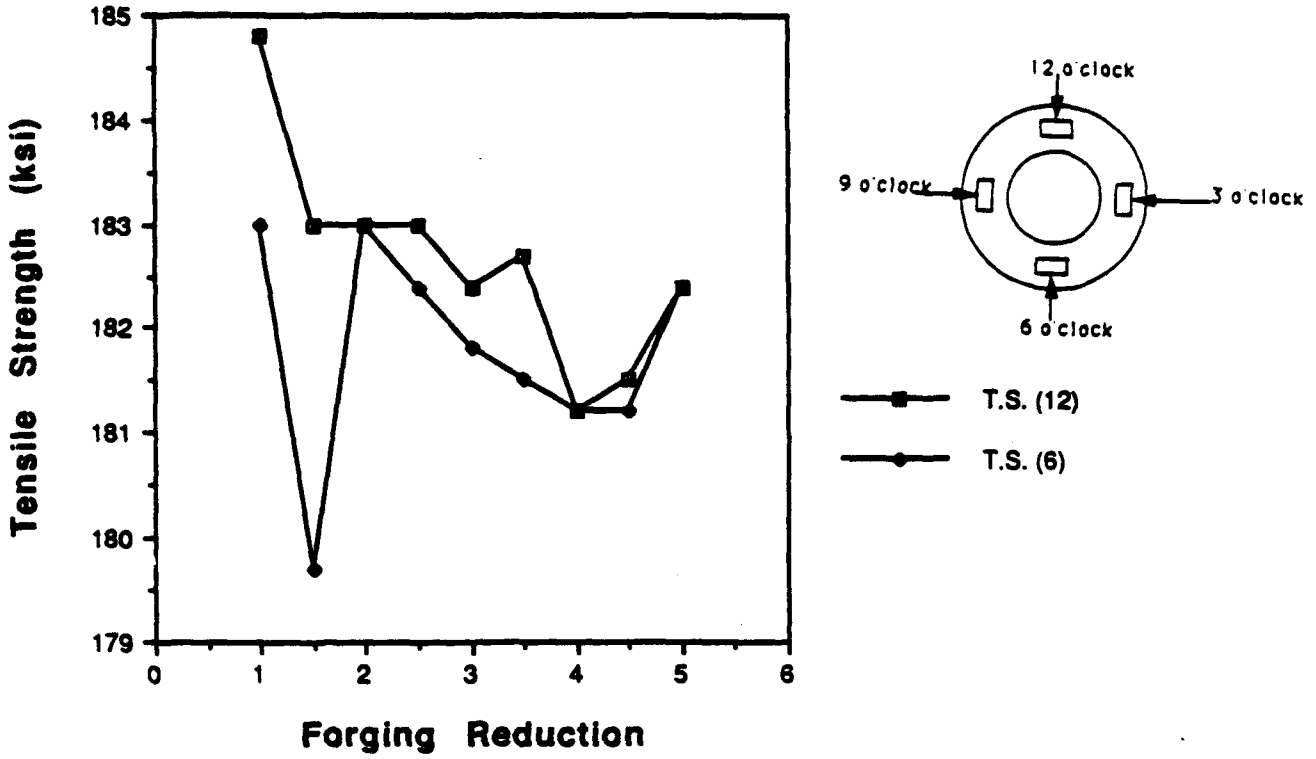

Figure 18. Tensile Strength Plot for AISI 4337 Steel.

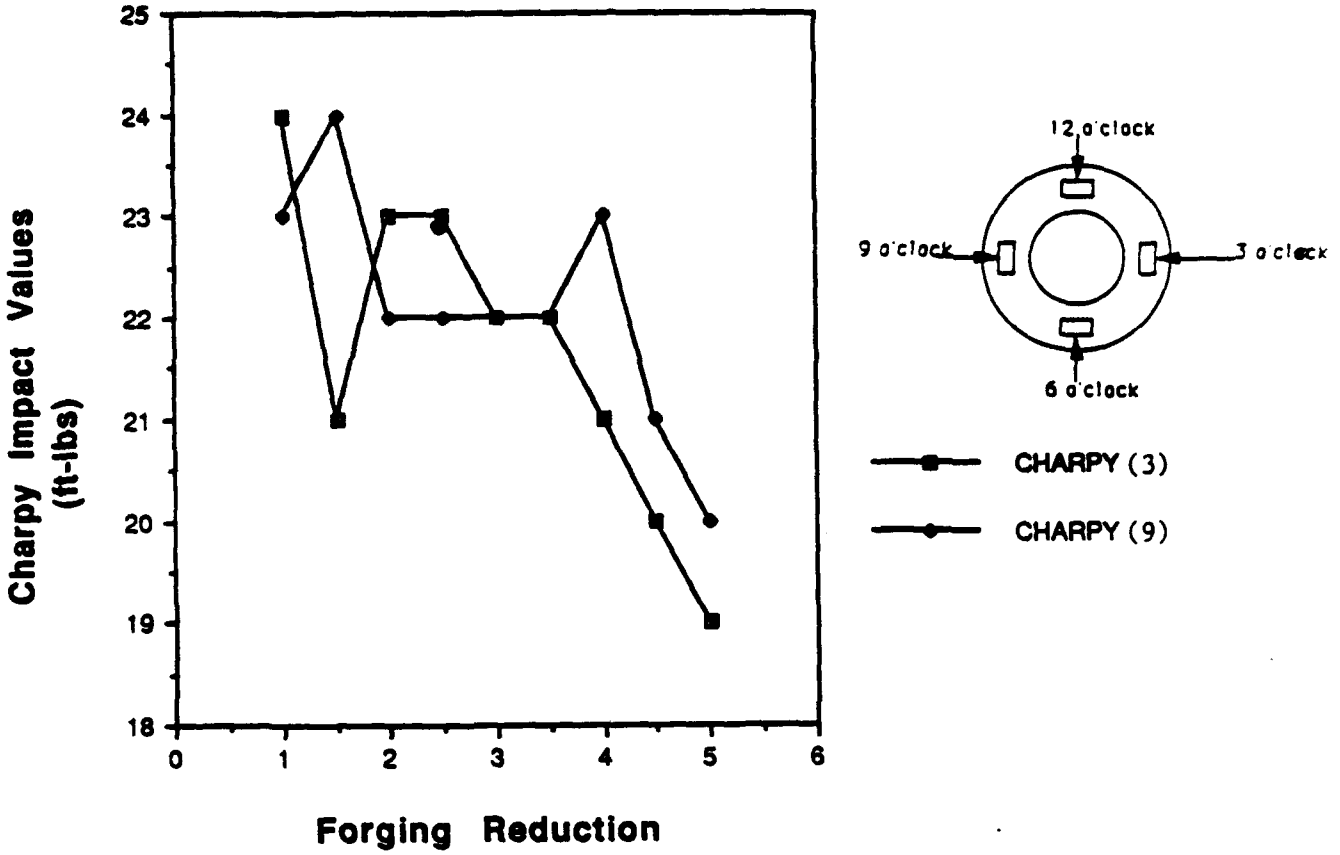

Figure 19. Charpy Impact Values for AISI 4337 Steel.

means of the data at each forging reduction are equal. Equivalently, it may be stated that there is no difference in a particular mechanical property as forging reduction is changed in the test under consideration. The alternative hypothesis states that the means of the data are not equal, hence the given mechanical property is affected by forging reduction.

Table 4. ANOVA Table for Yield Strength Test.

Source of Variation	D.O.F.	Sum of Squares	Mean Square	F
Reduction	8	11.320	1.415	2.339
Error	9	5.445	0.605	
Total	17	16.765		

Table 5. ANOVA Table for Tensile Strength Test.

Source of Variation	D.O.F.	Sum of Squares	Mean Square	F
Reduction	8	12.550	1.569	1.724
Error	9	8.190	0.910	
Total	17	20.740		

Table 6. ANOVA Table for Charpy Impact Test.

Source of Variation	D.O.F.	Sum of Squares	Mean Square	F
Reduction	8	22.778	2.847	2.847
Error	9	9.000	1.000	
Total	17	31.778		

As can be seen in Tables 4, 5, and 6, none of the F-test values were found to be greater than F(0.05,8,9). Hence the null hypothesis could not be rejected in any of the cases under consideration using the given data. That is to say that yield strength, tensile strength, and Charpy Impact Values are not greatly affected by the combined forging and heat treatment process being used. This does not totally eliminate the possibility that forging reduction does affect mechanical properties due to the large error terms found during the analysis. If the error terms could be reduced then the analysis would show that there is a significant effect between forging reduction and the mechanical properties. A large error term indicates that a large amount of random error is contained in the data. However, based on the results of the ANOVA tests in Tables 4, 5, and 6, it is not possible to design an optimum preform from the given data. Instead the problem requires additional study to eliminate the confounding effects of one process upon the other. To accurately determine whether the radial forging process affects the mechanical properties of AISI 4337 under the present forging conditions, a separate study is required. A recommended approach is to forge at temperature specimens of AISI 4337 at differing amounts of strain, air cool, and perform the required mechanical tests. The next step should be to separately investigate the effects of the heat treatment process on mechanical properties as material volume or forging reduction is varied using the same forging conditions in use at Watervliet. It is recommended that these issues be further studied prior to changing the present preform design. This is an important issue since the forging process is being carried out in the warm working range and the relative effects of work hardening and recovery on the resultant microstructure is not yet known.

Preform Design for Desired Product Properties

In the thermomechanical processing of alloys there are two basic philosophies that may be employed to yield a desired microstructure. The first approach is to produce the desired shape by any means possible and then use heat treatment to produce the desired microstructural properties (Ref. 27). The second approach is to tailor the mechanical processing at achieving the

preselected microstructure and abiding by the processing limitations imposed on temperature and percent reduction (Ref. 27). In this study the primary objective is to further the goal of achieving a desired microstructure during the radial forging process. Hence the latter approach will be employed.

This study is an effort to ensure that uniform mechanical properties are produced in forged gun tubes through application of uniform plastic deformation during the forging process. The primary focus is on Charpy Impact Data which indicates the relative toughness of the workpiece. In general, the toughness of a workpiece decreases with increasing amounts of cold work. However, production of gun tubes is normally carried out in the warm or hot working regions where the workpiece undergoes recovery and recrystallization during deformation. For this study a preliminary investigation of flow stress curves at warm working temperatures from a prior study by Battelle Columbus Labs (Ref. 25) showed a moderate increase in flow stress with increased deformation. It is well known that toughness is a function of grain size. For very small grain sizes, toughness increases with grain size to a maximum value after which toughness decreases with further increases in grain size. Hence, toughness is normally gained at the expense of strength under cold working conditions except when it is achieved through grain refinement (Ref. 28).

Grain Growth and Recrystallization Kinetics

Before describing the effects of deformation on the recrystallization process it is first helpful to describe recovery and recrystallization. Recovery is a process which acts to reduce the strain energy of the deformed material to a more thermodynamically stable state by eliminating both vacancies and dislocations without any subsequent rearrangement of the existing microstructure. As such, the original grain size is retained after recovery occurs. Another point that must be noted is that recovery occurs at a lower temperature than does recrystallization. Recrystallization also acts to reduce the strain energy imparted by deformation but accomplishes this through nucleation and growth of new, strain-free grains. This process occurs at a

higher temperature than does recovery. Before recrystallization can take place, a minimum amount of deformation or percent reduction must be imparted to the material.

The two processes may be considered to be in competition with one another in determining the final grain size. Once recovery or recrystallization has taken place, then it is not possible for the other process to occur. Both processes are dependent on the rate of heating as well as temperature (Ref. 29). If a slow rate of heating is used while heating to the recrystallization temperature then more recovery is able to occur as additional time is spent in the recovery region and more material will be reclaimed by this process. The reverse also applies to recrystallization.

It is well known that deformation affects the recrystallized grain size of most steels. Under cold working conditions the recrystallized grain size will decrease as percent strain increases during annealing. Therefore, it is clear that forging reduction is an important factor in controlling the resultant grain size. The initial grain size of the preform also influences the size of the recrystallized grain (Refs. 28,29). This may be seen by noting that new, recrystallized grains are nucleated at primarily at grain boundaries, triple junction points of boundaries, precipitates, and other points where regions of inhomogeneous plastic deformation exist to create high concentrations of strain energy which drive grain growth. In particular if a smaller grain size is present in the preform, more nucleation points will be available for recrystallization. To effectively control the final grain size of the gun tube and to optimize the forging process, it is necessary to determine at what temperatures that recovery and recrystallization occur for AISI 4337.

Effect of Deformation Parameters on Recrystallization

The importance of strain and strain rate on recrystallization must not be ignored as they directly impact the final grain size. The importance of strain rate may be described as follows. A larger strain rate enables higher processing or production rate. Heat loss to the dies and workpiece chilling is

also minimized (Ref. 28). The result of heat loss or chilling will obviously lower the billet temperature and cause a corresponding increase in the flow stress. In the radial forging process this would occur primarily at the inner and outer diameters of the tube at the tube/mandrel and tube/die interfaces. Moreover, this could lead to a non-uniform distribution of deformation across the tube wall which could ultimately affect the recrystallized grain structure. It is not anticipated that workpiece chilling due to die contact is significant due to the relatively short contact time. Heat loss by convection and radiation to the environment and to the water-cooled mandrel will be more significant. However, the heat losses may be compensated through proper selection of the stroking rate and feed rate. This is also favorable in that increased rate of heating minimizes recovery during deformation. However, the penalty for increased strain rate is that flow stress will also increase. This may be seen in the following well known power law relation:

$$\bar{\sigma} = C\dot{\bar{\varepsilon}}^{*} \tag{10}$$

The effect of strain may also influence the temperature of the workpiece. Intuitively as the amount of deformation is increased, greater amounts of work must be supplied to the billet. In plastic deformation processes, 95% of the added work will show up as heat in the form of temperature increase. Mathematically the change in temperature may be described as:

$$T_D = \frac{\bar{\sigma}\Delta\bar{\varepsilon}\beta}{Jc\rho} \tag{11}$$

(Ref. 7)

Hence larger strains will also tend to promote increases in temperature as does strain rate.

Effect of Grain Refiners on Recrystallization

Another possibility which exists for controlling the grain size in the forging is to investigate the introduction of stable second phase particles or

grain refiners into the steel matrix. Second phase particles are commonly used to control grain size in aluminum killed steels and aluminum alloys. The grain refiners are most effective when they are dispersed in a fine, even distribution throughout the matrix where they act as a drag against expanding grain boundaries. In order for the grain boundaries to continue expanding, additional energy must be available to the grain boundary (Refs. 28,29). The effect of the second phase particle size on final recrystallized grain diameter may be seen in the Zener-Holoman equation below. Caution must be exercised when the material is heated to avoid the reversion temperature of the particles at which they will dissolve back into solution and permit discontinuous grain growth to take place.

(12) $D_{gr} = \frac{4r_p}{3v_f}$ (Ref. 28)

Preform Development

The present preform shape being used at Watervliet is shown below in Figure 20. The new preform design will be developed using the concept of constant volume during plastic deformation. The concept of constant volume in plastic deformation processes is based on the fact that when all strain components are added together the result is zero which indicates that no change in workpiece volume has occurred. This is written mathematically in Cartesian coordinates as:

(13) $\varepsilon_{xx} + \varepsilon_{yy} + \varepsilon_{zz} = 0$

Here ε_{ii} is defined as true or logarithmic normal strain as in equation 14:

(14) $\varepsilon_{ii} = \ln \frac{\text{final dimension}}{\text{initial dimension}}$

Although the subscripts xx, yy, zz are commonly used in many forming analyses, the polar coordinate system is more commonly employed in studies

involving prismatic or rotational workpieces involving circular and/or tubular cross-sections. The notation for polar coordinates is as follows: ε_{rr}, $\varepsilon_{\theta\theta}$, ε_{zz} corresponding to the radial, tangential, and axial directions as shown below in Figure 21. The strains are calculated as follows (Ref. 30):

$$\varepsilon_{rr} = \ln\left(\frac{R_{of} - R_{if}}{R_o - R_i}\right) \tag{15}$$

$$\varepsilon_{\theta\theta} = \ln\left(\frac{R_{of} + R_{if}}{R_o + R_i}\right) \tag{16}$$

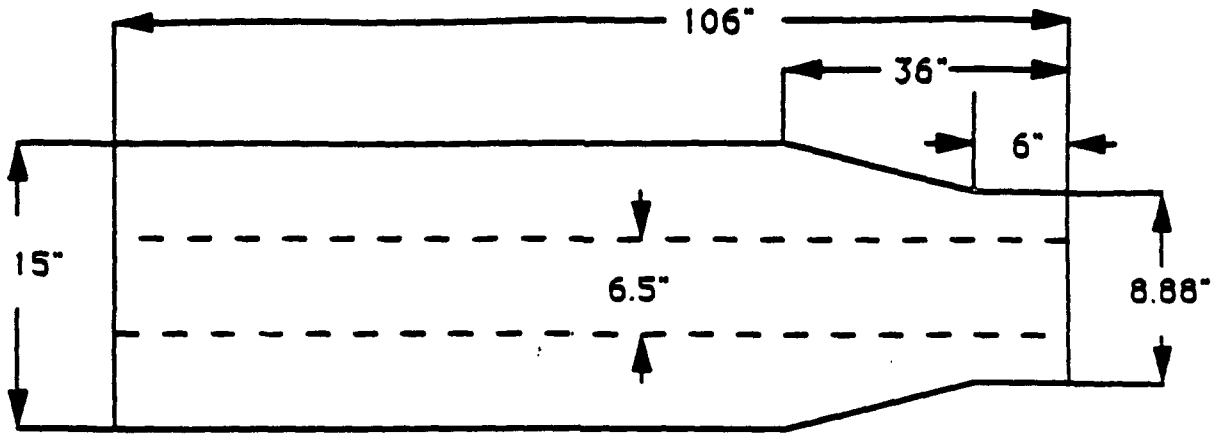

Figure 20. Experimental Preform Design (Ref. Sketch 7-89).

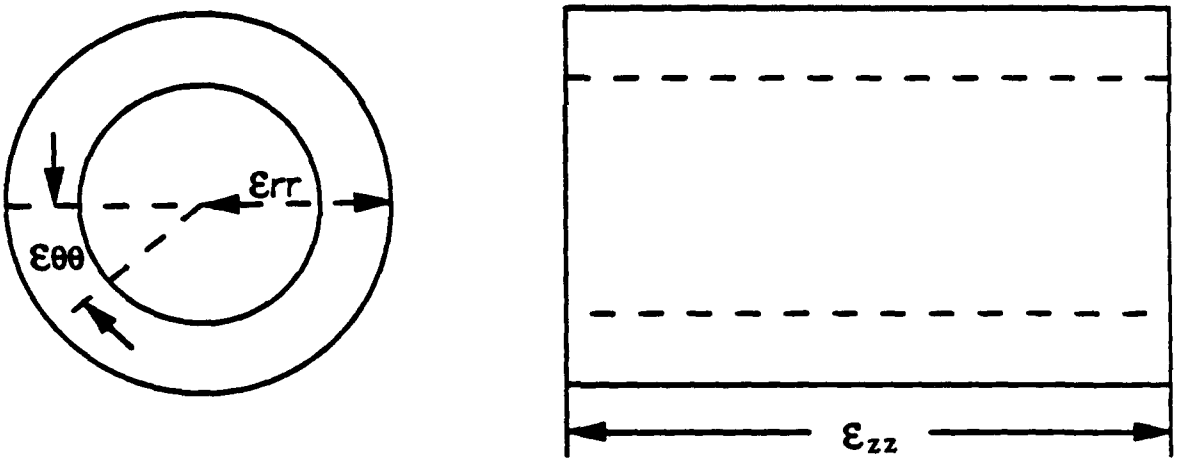

Figure 21. Polar Coordinate Notation.

(17) $\varepsilon_{zz} = -(\varepsilon_{rr} + \varepsilon_{\theta\theta})$ from constant volume

alternatively ε_{zz} may be expressed as :

(18) $\varepsilon_{zz} = \ln \frac{z_f}{z_i}$

To facilitate the analysis, the finish forged gun tube was divided into three geometrically distinct regions as shown below in Figure 22. It was planned to calculate the strains from the muzzle end of the gun tube as the data indicated that the highest Charpy Impact values were found at the muzzle. This implied that as for the as-received preform, that minimum deformation and the subsequent heat treatment yielded the highest toughness. However upon analyzing the strains at the muzzle end it was found that due to the small amount of deformation applied, the wall thickness had increased (i.e. positive value of ε_{rr}). This condition is often observed in tube sinking for low values of friction and reduction (Ref. 30). However as these conditions would be applicable only during deformation at the muzzle end, applying the same conditions throughout the workpiece would not yield a satisfactory design for the preform. Therefore, it was decided to use the reduction at the breech end to calculate the strains for the preform as this was felt to be more representative of the overall forging conditions. It should be noted that a different preform could be designed to optimize the microstructure for recrystallization by simply replacing the values of ε_{rr}, $\varepsilon_{\theta\theta}$, and ε_{zz} with the desired values of reduction and repeating the calculations shown below. It was assumed during the analysis that sufficient deformation would be available during forging to drive recrystallization. However this should be verified with the material vendor as this information was not available.

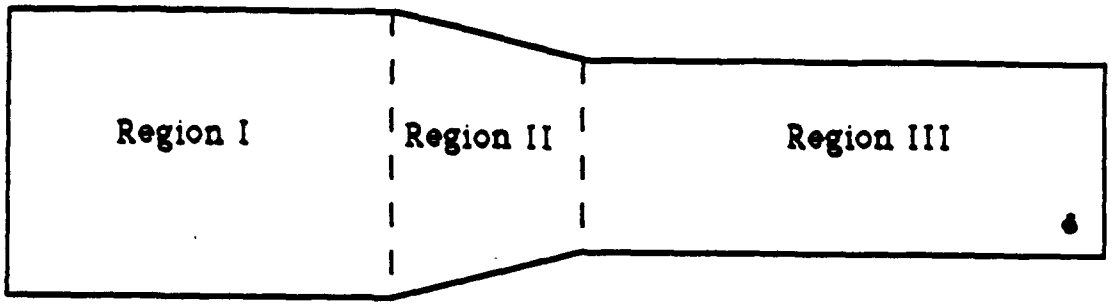

Figure 22. Definition of Geometric Regions.

Calculating the strain at the breech end the calculations are shown below:

(19) $$\varepsilon_{rr} = \ln \frac{6.225 - 2.660}{7.500 - 3.250} = -0.176$$

(20) $$\varepsilon_{\theta\theta} = \ln \frac{6.225 + 2.660}{7.500 + 3.250} = -0.191$$

(21) $$\varepsilon_{zz} = -(-0.178 - 0.191) = 0.367$$

Now applying this to the preform to determine the axial length, z_i of the preform:

(22) $$z_i = \frac{z_f}{\exp(0.367)}$$

Using z_f = 82.5 inches from Figure 20, z_i = 57.157 inches.

To perform a similar analysis for the muzzle end, it must be noted that to solve for the preform dimensions that the equation is a function of two variables: R_o and R_i. This is solved by noting that the internal bore for the

preform will be the same throughout: 6.500 inches. Using a similar analysis as in equation 19 for the breech end of the preform the following values are obtained:

$$(23) \quad \ln \frac{4.025 - 2.660}{R_o - 3.250} = -0.176$$

solving for R_o, R_o = 4.880 inches. Similarly for the preform length:

$$(24) \quad \ln \frac{82.500}{z_i} = 0.367$$

which leads to the result that z_i = 64.431 inches.

For Region II the preform dimensions can be calculated by noting the fact that the volume of the preform and the forging are equal and that the inner and outer radii of the preform at the entrance and exit of Region II are equal to those of Region I and III respectively. Hence the problem reduces to that of equating the volumes of the preform and the workpiece and solving for z_i. The equation for the volume of a frustum is:

$$(25) \quad \text{Volume} = \frac{\pi[r^2 + rR + R^2]h}{3}$$

where r, R, and h are shown in Figure 23. To account for the internal bore of the workpiece, the volume of a right circular cylinder is subtracted:

$$(26) \quad \text{Volume} = \pi r^2 l$$

where r is the radius of the cylinder and l is the length.
Writing the equation, volume preform^{II}= volume forging^{II}:

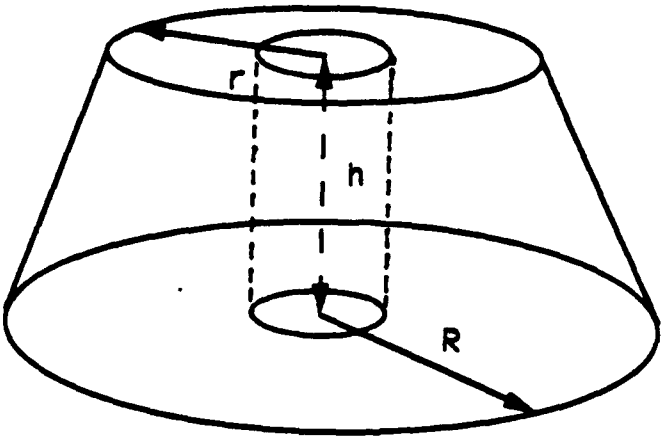

Figure 23. Notation for Calculation of Frustum Volume.

$$(27)\quad (7.500^2 + 4.880 \times 7.500 + 4.880^2)\, z_i \frac{\pi}{3} - \pi(3.250)^2 z_i =$$

$$(6.225^2 + 4.025 \times 6.225 + 4.025^2) 30 \frac{\pi}{3} - \pi(2.660)^2 30$$

z_i is found to be: 20.752 inches. The resulting preform design is shown below in Figure 24.

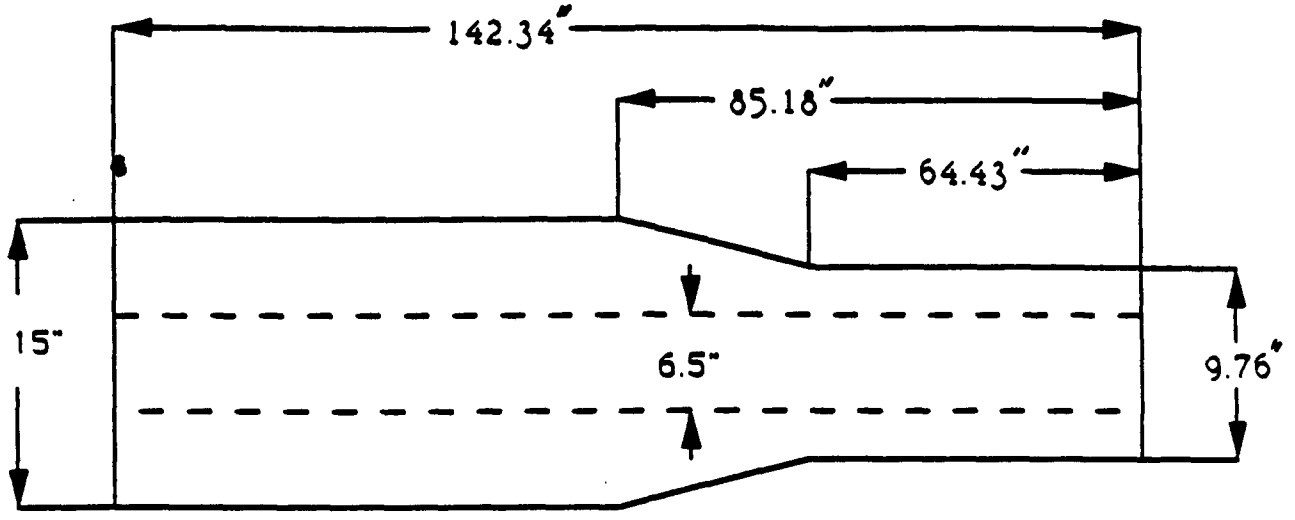

Figure 24. New Preform Design for Watervliet Arsenal.

CONCLUSIONS

In comparison with other forging processes, the state of radial forging process analysis has not been highly developed. Of the forming models which have been presented, most rely on the approximation that the process may be modeled as a variation of extrusion. While this approximation greatly facilitates the mathematical modeling of radial forging, it does not accurately reflect the metal flow and friction conditions which have different signs on either side of the neutral plane as in upsetting. With the advent of FEM programs such as ALPID and DEFORM, radial forging process modeling has been greatly facilitated and all conditions are easily simulated, including forging of hollow and solid workpieces. However, a true simulation of the physical process can not be made until new three-dimensional FEM software becomes available and accurate flow stress data for metals at warm and hot working temperatures is generated.

1. In this study RFORGE and DEFORM were used to perform radial forging simulations. DEFORM was found to be superior to RFORGE for simulating a wide variety of process conditions but neither was found to be useful in preform design.

2. Deformation conditions during radial forging have a direct effect on the resulting microstructure of the forged tube. However due to probable confounding effects from heat treatment, no effect was noted on the mechanical properties with varying reduction.

3. The effects of the radial forging and heat treatment processes should be studied independently to ascertain their effect on the microstructure of the gun tube.

4. For the preform design, simple plastic strain calculations and concepts were used to develop the design presented in Figure 24. It is recommended that the true strain concept be adopted for describing the forging reduction.

REFERENCES

1. Lange, K., "NC-Radial Forging- A New Concept in Flexible Automated Manufacturing of Precision Forgings In Small Quantities", Proceedings of 1st International Machine Tool Design and Research Conference, April 1985, Birmingham, pp. 63-72.

2. Wohr, A., Lange, K., "NC-Radial-Forging - Present State and Further Development", Advanced Technology of Plasticity, Vol. 11, 1986, pp. 1119-1131.

3. Green, M.G., and Pick, R., "The Open-Die Forge Press-Today and Tomorrow", SMS Hasenclever Sales Literature, 1988.

4. Altan, T., Boulger, F.W., Becker, J.R., Akgerman, N., and Henning, H.J., Forging Equipment, Materials, and Practices, Publication #MCIC-HB-03, Battelle Columbus Laboratories, October 1973, pp. 58-63.

5. Hojas, H., "Radial Forging", American Society for Metals Handbook, Vol. 14, 9th ed., 1988, pp. 195.

6. American GFM Corp. Sales Literature, Chesapeake, VA, 1990.

7. Altan, T., Oh, S., Gegel, H., Metal Forming Fundamentals and Applications, American Society for Metals, 1983, p. 90,166.

8. Fenn Forging Machines Sales Literature, 1987.

9. Selwood, R.W., "Ruthner Hydraulic Forging Machine", FIA Forging Equipment Symposium, June 1982, Chicago.

10. Selwood, R.W., "GFM Automatic Die Forging Machine", SME Technical Paper MF72-532, 1972.

11. SMS Hasenclever Technical Literature CNC Radial Forging, 1986, p. 7.

12. GFM Precision Forging Machines, Technical Literature, 9/8/76, p.10.

13. Kilpatrick, W., Rotary Forge Fills Specialty Needs", Mechanical Engineering, February, 1984, pp. 30-33.

14. Liuzzi, L., Heiser, F., Campione, A., Cold Rotary Forging, U.S. Army Report #WVT-TR-T5054, September, 1975.

15. Lahoti, G.D., Altan, T., Analysis and Optimization of the Radial Forging Process for Manufacturing Gun Barrels, U.S. Army Report, September 1974, pp. 12,A8.

16. Ragupathi, P.S., Lahoti, G.D., Altan, T., Application Of The Radial Forging Process To Cold And Warm Forging of Cannon Tubes, Volume III: Analysis of Stresses In The Mandrel, U.S. Army Report, May 1980, pp. 1-27.

17. Nagpal, V., Lahoti, G.D., Application Of The Radial Forging Process To Cold And Warm Forging of Cannon Tubes, Volume II: Selection of Die and Mandrel Materials, U.S. Army Report, May 1980, pp. 55-65.

18. Sachs, G., and Baldwin, M., "Stress Analysis of Tube Sinking", Journal of Engineering for Industry, American Society of Mechanical Engineers, November 1946, pp. 655-662.

19. Kegg, R.L., "Mechanics of the Rotary Swaging Process", Journal of Engineering for Industry, American Society of Mechanical Engineers, November 1964, pp. 317-325.

20. Lange, K., "Cost Minimization in Small Quantity Production of Stepped Shafts by Combined NC Radial Forging and NC Turning - A New Approach to Flexible Manufacturing Systems", Annals of the CIRP, Vol. 34/2/1985, pp. 549- 555.

21. Paukert, R., "Investigations Into Metal Flow In Radial Forging", Annals of the CIRP, Vol. 32/1/1983, pp. 211-217.

22. Isogawa, S., Suzuki, Y., Uehara, N., "Temperature Transition and Deformation Process of Inconel 718 During Rotary Forging", Internal Paper, Central Research Lab, Daido Steel Company, pp. 7-9.

23. Im, Y., Dudra, S.P., Analysis of Metal Flow in Massive Hot Open-Die Forging, ERC/NSM-88-10, July, 1988, pp. 7-11.

24. Hojas, H., "Hot and Cold Forging With 4 Hammer Precision Forging Machines", GFM Ges.m.b.h., Steyr, Austria, pp. 11-12.

25. Lahoti, G.D., Subramanian, T.L., Altan, T., Analysis and Optimization of the Radial Forging Process for Manufacturing Gun Barrels: Phase III- Optimization of the Process, U.S. Army Report, April 1977, Appendix B.

26. Devore, J., Probability and Statistics for Engineering and the Sciences, Brooks/Cole Publishing Co., 1987, pp. 368-377.

27. Sims, C.T., Hagel, W.C., The Superalloys, J. Wiley and Sons, New York, 1972, pp. 461-466.

28. Backofen, W.A., Deformation Processing, Addison-Wesley, 1972, pp. 265-286.

29. Shewmon, P.G., Transformations in Metal, J. Williams Book Co., OK, 1983, pp. 69-125.

30. Avitzur, B., Metal Forming Processes and Analysis, TATA McGraw-Hill TMH ed., 1977, pp. 341-352.

APPENDIX A: RFORGE USER'S MANUAL

DESCRIPTION OF THE COMPUTER PROGRAM RFORGE

During Phase I and Phase II of this development study on the "Analysis and Optimization of the Radial-Forging Process for Manufacturing Gun Barrels", three sets of computer programs were developed. The first set, named RADFLW, determines a kinematically-admissible upper-bound velocity field, strains, strain rates, and an upper bound on the total forging load in radial forging of gun barrels over a stationary mandrel. The second set of programs called RFTEMP, uses the velocity field data generated by RADFLW to obtain temperature distributions in the billet, the mandrel, the die and the product in radial forging of tubes. The third set of programs, named RFCOMP, determines the stresses and loads in radial forging of gun barrels or tubes using the compound angles, and it is also valid for dies with single-entrance angle.

For overall optimization of the radial-forging process, all these three sets of programs are grouped together under the name RFORGE. In this modified form, any desired information, such as upper-bound velocity field, strains, strain rates, temperature distributions or the load and pressure on the dies, can be generated with one set of input data. Thus, with the use of RFORGE, generating data to plot performance curves is relatively simple, and the process optimization for a given set of input conditions can be easily established with a minimum number of computer runs.

All the routines in RFORGE have been coded as subroutines or subfunctions. Hence, they can be used in a simple one-line structure or in an overlay structure. Since the memory space requirements for the one-line structure of the RFORGE exceeded the capacity of the IBM-360 computer at the Watervliet Arsenal, an overlay structure, as depicted in Figure B-1, was developed. In its present overlay form, RFORGE requires 19C88 (hexadecimal) or 81000 (decimal) memory locations. Since the overlay structure is established by a set of control cards, modification of the structure due to the addition or deletion of subroutines requires minimum effort.

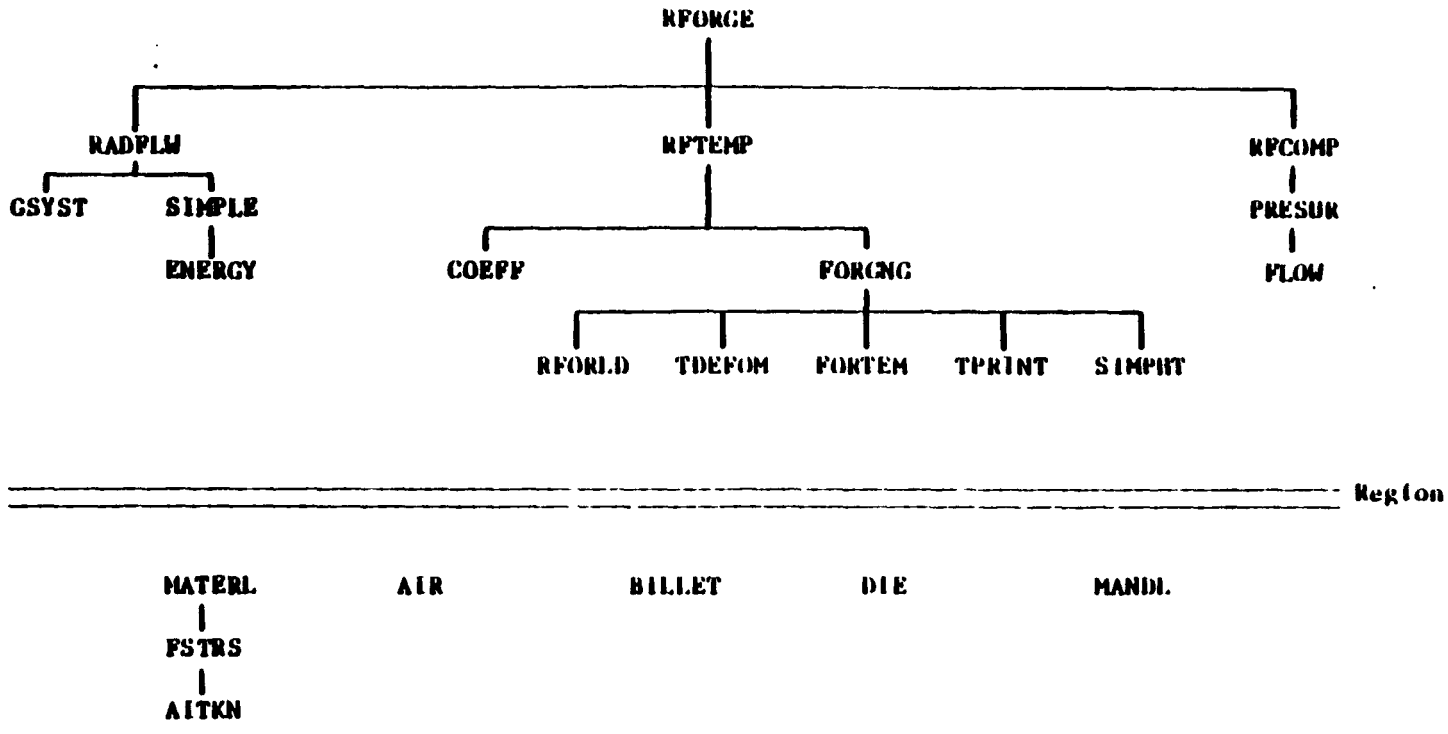

FIGURE B-1. OVERLAY STRUCTURE OF THE SET OF COMPUTER PROGRAMS RFORGE

Input to and Output from Program RFORGE

All process variables are read by RFORGE. In addition, the choice to compute one or more of (a) upper-bound velocity field, (b) temperature distributions in the billet, the mandrel, the die and the product, and (c) load and pressure on the dies, are read in as input. The process variables being read include:

(a) The dimensions of the preform and of the forged barrel

(b) The dimensions and the velocities of the forging dies

(c) The values of friction at die material and mandrel-material interfaces

(d) The magnitudes of back push, front pull, and axial feed

(e) Initial temperature and type of the metal being forged.

The flow stress of the forged material for given values of strain, strain rate, and temperature are obtained by interpolation from the tabulated flow stress data, included in the program.

RFORGE, which coordinates the functions of all other major routines, also prints out the data read in. After the initialization of some of the input values, the major routines RADFLW, RFTEMP, and RFCOMP are called as prescribed by the user during the input procedure.

Input Preparation for RFORGE(*)

(The quantity in parentheses, following the description of each input variable, represents an example input).

1. First Card, Format (3L10,I10)

Columns 1-10: A(*), Logical (TRUE or FALSE) input to indicate whether velocity field is to be generated. A 'T' in anyone of the first 10 columns will set this variable to TRUE. An 'F' or all blanks will set it to FALSE. (T)

(*) See Figure B-2 for variable names used here.

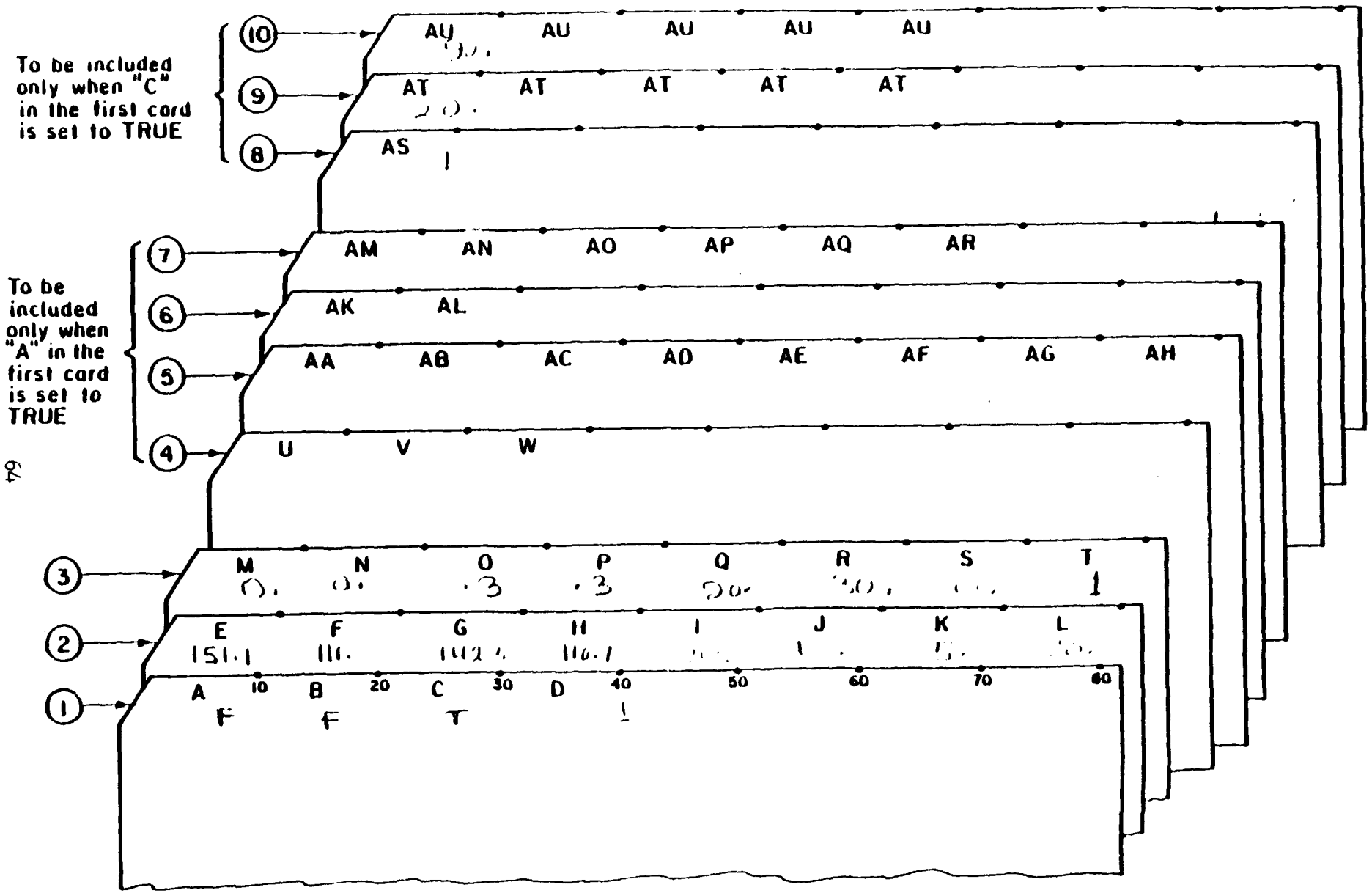

FIGURE B-2. INPUT DATA STRUCTURE

11-20: B. Logical (TRUE or FALSE) input to indicate whether the elaborate temperature distributions are to be computed. Since velocity field is needed for the computation of temperature distribution, the first variable must also be set to true, when this variable is assigned true. When the first variable is set to TRUE and the second variable is set to FALSE, an average temperature of the deformation zone, heat generated by metal deformation, heat absorbed by deforming material, heat lost by conduction, convection and radiation are calculated by approximate heat transfer formulas. (T)

21-30: C, Logical (TRUE or FALSE) input to indicate when load and pressure estimations are to be performed. (T)

31-40: D, An integer used to print out intermediate results. When set to zero, only the final results will be printed. Input data and final results will be printed when set to 1. All other variables that will be printed for a higher setting of this variable are shown in Table B-2 attached at the end. Maximum value for IPRINT is 9. Faulty setting of 10 or more will automatically be reduced to 1. (3)

2. Second Data Card, Format (8F10.3)

Columns 1-10: E, Outside diameter of the tubular preform, mm (560.)

11-20: F, Inside diameter of the tubular preform, mm (318.)

21-30: G, Outside diameter of the forged product, mm (353.)

31-40: H, Inside diameter of the forged product, mm (287.)

41-50: I, Length of the die land, mm (165.)

51-60: J, Radial velocity of the forging tools, mm/sec (180.)

61-70: K, Axial feed of the preform, mm/stroke (10.)

71-80: L, Entrance angle of the forging tools, degrees (15.)

3. Third Data Card, Format (7F10.3, I10)

Columns 1-10: M, Back-pull force (negative, if back push), kN (0.)
11-20: N, Front-pull force (negative, if front push), kN (0.)
21-30: O, Friction shear factor between tube and die (0.6)
31-40: P, Friction shear factor between tube and mandrel (0.5)
41-50: Q, Initial uniform temperature of the billet, C (1000.)
51-60: R, (β) angle of contact for a round-faced tool, degrees. (See Figure B-3, optional for a flat-faced tool) (90.)
61-70: S, (γ) angle of tangency of a flat-faced tool, degrees. (See Figure B-4, optional for a round-faced tool) (0.)
71-80: T, A code for type of tool (1)
1 for round-faced tool
2 for flat-faced tool.

As an example, the input data, as printed by the program RFORGE, are shown in Figure B-5. The program prints these input data so that input can be checked for possible errors.

RFORGE reads the data continuously until the end of file is encountered. Hence, for process optimization, any number of data sets can be read in a single run.

The following data card should not be included in the input data stream, if the first variable (A) in the input list to RFORGE is set to FALSE.

4. Fourth Card, Format (3I10)

Columns 1-10: U, Number of radial divisions on the entrance side (15)
11-20: V, Number of axial divisions (12)
21-30: W, Number of radial divisions on the exit side (5)

As an example, the input data, as printed by the program RADFLW, are given in Figure B-6. The sample output for the same input data is given in Figure B-7.

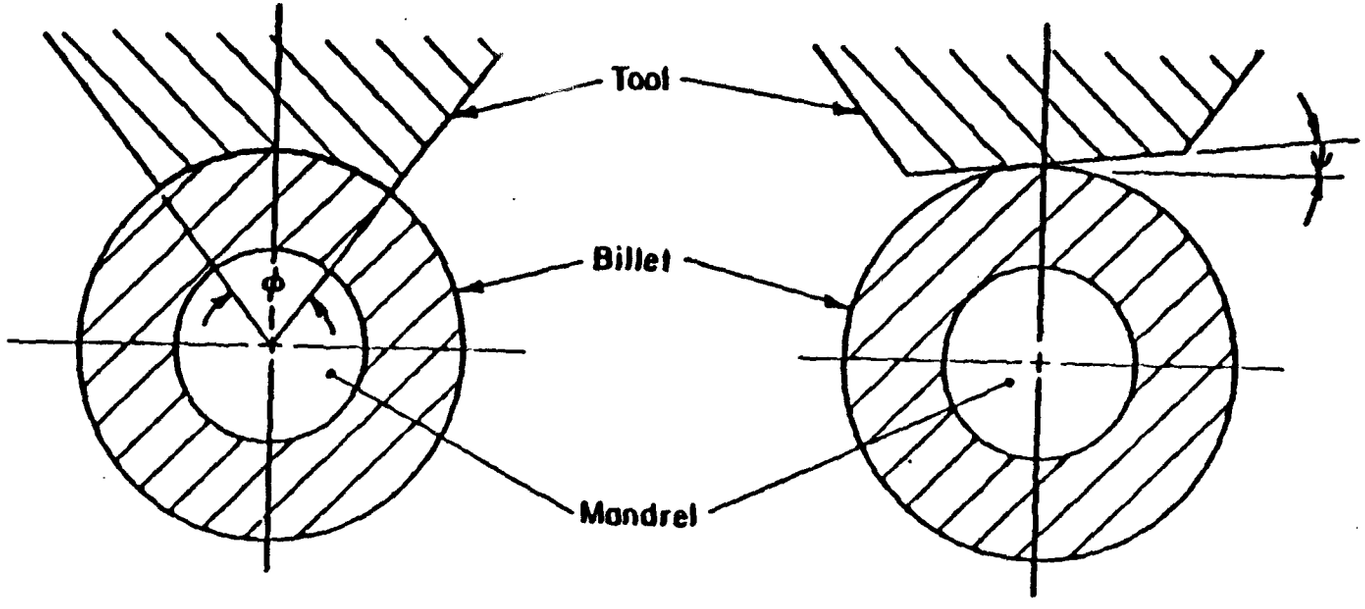

FIGURE B-3. ANGLE OF CONTACT FOR A ROUND-FACED TOOL

FIGURE B-4. ANGLE OF TANGENCY FOR A FLAT-FACED TOOL

INPUT TO RFORGE		
LOGICAL VARIABLE TO EXECUTE VELOCITY PROGRAM,F	=	T
LOGICAL VARIABLE TO EXECUTE TEMPERATURE PROGRAM,F	=	T
LOGICAL VARIABLE TO EXECUTE PRESSURE PROGRAM,F	=	T
INDEX TO PRINT INTERMEDIATE RESULTS,I	=	3
OUTSIDE DIAMETER OF THE TUBULAR PREFORM,MM	=	540.00
INSIDE DIAMETER OF THE TUBULAR PREFORM,MM	=	318.00
OUTSIDE DIAMETER OF THE FORGED PRODUCT,MM	=	353.00
INSIDE DIAMETER OF THE FORGED PRODUCT,MM	=	247.00
LENGTH OF THE DIELAND(SIZING ZONE),MM	=	165.00
RADIAL VELOCITY OF THE FORGING TOOLS,MM/SEC	=	180.00
AXIAL FEED OF THE PREFORM,MM/STROKE	=	10.00
ENTRANCE ANGLE ON THE FORGING TOOLS,DEGREES	=	15.00
BACK PULL(WITH A NEGATIVE SIGN,IF BACK PUSH),KN	=	0.00
FRONT PULL(WITH A NEGATIVE SIGN,IF FRONT PUSH),KN	=	0.00
FRICTION SHEAR FACTOR BETWEEN DIE AND TUBE	=	.60
FRICTION SHEAR FACTOR BETWEEN MANDREL AND TUBE	=	.50
INITIAL UNIFORM TEMPERATURE OF THE BILLET,C	=	1000.00
TOOL CONTACT ANGLE (FOR ROUND TOOLS ONLY),DEGREES	=	90.00
TOOL TANGENCY ANGLE(FOR FLAT TOOLS ONLY),DEGREES	=	0.00
TYPE OF FORGING TOOL DIE-FACE	=	ROUND

FIGURE B-5. SAMPLE INPUT DATA AS PRINTED BY RFORGE

INPUT TO THE PROGRAM RADFLW

NUMBER OF RADIAL DIVISIONS ON ENTRY SIDE	=	15
NUMBER OF TOTAL AXIAL DIVISIONS	=	12
NUMBER OF RADIAL DIVISIONS ON EXIT SIDE	=	5

FIGURE B-6. SAMPLE INPUT DATA AS PRINTED BY RADFLW PRIOR TO PERFORMING COMPUTATIONS

OUTPUT FROM THE PROGRAM RADFLW

LENGTH OF THE FORGING ZONE, MM	=	.736267E+03
DISTANCE OF THE NEUTRAL PLANE FROM ENTRY, MM	=	.736267E+03
AVERAGE STRAIN IN THE FORGING ZONE, M/M	=	.171005E+01
AVERAGE STRAIN-RATE IN THE FORGING ZONE, 1/S	=	.116453E+01
AVERAGE FLOW STRESS, MN/SQ.M	=	.192936E+03
TOTAL RADIAL FORGING LOAD PER TOOL, N	=	.451932E+05
AVERAGE RADIAL FORGING PRESSURE, MN/SQ.M	=	.253301E+03
ENERGY RATE SUPPLIED BY TOOLS, MM/S	=	.325391E+08

GZ(J) = AXIAL COORDINATE OF A GRID POINT, MM
GR(I) = RADIAL COORDINATE OF A GRID POINT, MM
UZ(I,J) = AXIAL COMPONENT OF VELOCITY, MM/SEC
UR(I,J) = RADIAL COMPONENT OF VELOCITY, MM/SEC
SR(I,J) = EFFECTIVE STRAIN-RATE, 1/SEC

I	J	GZ(J)	GR(I)	UZ(I,J)	UR(I,J)	SR(I,J)
1	1	0.	.1435E+03	-.5491E+03	0.	.3578E+00
2	1	0.	.1511E+03	-.5491E+03	-.2056E+01	.3612E+00
3	1	0.	.1587E+03	-.5491E+03	-.4029E+01	.3540E+00
4	1	0.	.1633E+03	-.5491E+03	-.5925E+01	.3491E+00
5	1	0.	.1699E+03	-.5491E+03	-.7756E+01	.3450E+00
6	1	0.	.1765E+03	-.5491E+03	-.9529E+01	.3417E+00
7	1	0.	.1841E+03	-.5491E+03	-.1221E+02	.3378E+00
8	1	0.	.1972E+03	-.5491E+03	-.1478E+02	.3350E+00
9	1	0.	.2075E+03	-.5491E+03	-.1725E+02	.3332E+00
10	1	0.	.2179E+03	-.5491E+03	-.1965E+02	.3319E+00
11	1	0.	.2282E+03	-.5491E+03	-.2198E+02	.3311E+00
12	1	0.	.2386E+03	-.5491E+03	-.2426E+02	.3308E+00
13	1	0.	.2489E+03	-.5491E+03	-.2648E+02	.3307E+00
14	1	0.	.2593E+03	-.5491E+03	-.2865E+02	.3310E+00
15	1	0.	.2696E+03	-.5491E+03	-.3079E+02	.3314E+00
16	1	0.	.2800E+03	-.5491E+03	-.3288E+02	.3321E+00
1	2	.3863E+02	.1475E+03	-.5357E+03	0.	.4358E+00
2	2	.3863E+02	.1511E+03	-.5357E+03	-.2436E+01	.4257E+00
3	2	.3863E+02	.1587E+03	-.5357E+03	-.4772E+01	.4195E+00
4	2	.3863E+02	.1633E+03	-.5357E+03	-.7019E+01	.4136E+00
5	2	.3863E+02	.1699E+03	-.5357E+03	-.9189E+01	.4098E+00

FIGURE B-7. PARTIAL SAMPLE OUTPUT FROM RADFLW FOR THE INPUT DATA GIVEN IN FIGURES B-5 and B-6

The following three data cards should be included in the input data stream only when the first variable (A) in the input list to RFORGE is set to TRUE (T).

5. Fifth Data Card, Format (8F10.4)

Columns 1-10: AA, Diameter of the cooling pipe in mandrel, mm (30.)
11-20: AB, Effective length of the mandrel, mm (200.)
21-30: AC, Length of the tubular preform, mm (200.)
31-40: AD, Number of forging strokes, per minute (200.)
41-50: AE, Fraction of stroke while tools contact material (0.5)
51-60: AF, Initial temperature of the die, C (50.)
61-70: AG, Initial temperature of the mandrel, C (50.)
71-80: AH, Temperature of the mandrel coolant, C (50.)

6. Sixth Data Card, Format (8F10.4)

Columns 1-10: AK, Ambient temperature, C (20.)
11-20: AL, Scale thickness between the billet and mandrel, mm (0.)

7. Seventh Data Card, Format (8I10)

Columns 1-10: AM, Limiting number of iterations per grid movement of the billet (20)
11-20: AN, Transverse grid lines where simulation stops (19)
21-30: AO, Number of desired iteration for debugging purpose. Leave blank otherwise.(0)
31-40: AP, Number of transverse grid lines in the billet (12)
41-50: AQ, Number of longitudinal grid lines in the mandrel (5)
51-60: AR, Number of longitudinal grid lines in the dies (4)

As an example, the input data, as printed by program RFTEMP, are shown in Figure B-8. The sample output for the same input data is given in Figure B-9. Figure B-9a is a partial output after extensive heat transfer analysis. (When the second variable B, of the first card is set "TRUE"). Figure B-9b is the output obtained after simplified heat transfer analysis. (When the second variable B of the first card is set to "FALSE").

INPUT TO THE PROGRAM RFTEMP		
DIAMETER OF THE COOLING PIPE IN MANDREL,MM	=	38.00
EFFECTIVE LENGTH OF THE MANDREL,MM	=	200.00
LENGTH OF THE TUBULAR PREFORM,MM	=	200.00
NUMBER OF FORGING STROKES PER MINUTE	=	200.00
AMBIENT TEMPERATURE,C	=	20.00
INITIAL UNIFORM TEMPERATURE OF THE TOOLS,C	=	90.00
INITIAL UNIFORM TEMPERATURE OF THE MANDREL,C	=	90.00
TEMPERATURE OF THE MANDREL COOLANT,C	=	90.00
NO. OF RADIAL GRID LINES IN THE BILLET	=	12
NO. OF AXIAL GRID LINES IN THE MANDREL	=	9
NO. OF AXIAL GRID LINES IN THE TOOLS	=	4
NUMBER OF THE RADIAL GRIDLINE WHERE SIMULATION END=		19
THICKNESS OF SCALE BETWEEN MANDREL AND TUBE,MM	=	0.000
FRACTION OF STROKE DURING WHICH TOOL CONTACT WAS=		.500

FIGURE B-8. SAMPLE INPUT DATA AS PRINTED BY RFTEMP PRIOR TO PERFORMING TEMPERATURE CALCULATIONS

```
THE FOLLOWING RESULTS ARE
 AT THE END OF ITERATIONS                7
 WHEN BILLET FRONT IS AT                 1
 WHEN BILLET END  IS AT                 24
 WHEN PRODUCT LENGTH HAS                 5  GRIDS
 TIME ELAPSED IS                    .5600  SECONDS

 FORGING POWER PER TOOL          6795.3599  KW

 FORGING LOAD PER TOOL             37.7520  MN

 TEMPERATURE DISTRIBUTIONS IN THE PRODUCT,BILLET,DIE, AND MANDREL ARE GIVEN BELOW

 IN EVERY LISTING, VALUES FROM LEFT TO RIGHT ARE TEMPERATURES
 IN THE RADIAL DIRECTION FROM AXIS TO OUTER SURFACE

 THE FIRST LINE IN EVERY LISING REFERS THE DESIGNATIONS OF THE HORIZONTAL LINES AND
 THE SECOND LINE GIVES THEIR DISTANCES IN MM FROM THE AXIS

 THE FIRST NUMBER IN EVERY LINE IS THE DESIGNATION OF THE VERTICAL LINE AND
 THE SECOND NUMBER IS ITS AXIAL DISTANCE IN MM FROM DIE EXIT


 TEMPERATURE DISTRIBUTION IN THE PRODUCT FROM PRODUCT END TO DIE EXIT

                      1       2       3       4       5       6       7       8       9      10
                   0.00   15.00   47.13   79.25  143.58  156.18  156.78  163.38  169.98  176.58

  32-183.000      20.0    20.0    20.0    20.0   532.4   943.7   996.7   996.6   946.6   625.7
  31 -83.333      20.0    20.0    20.0    20.0   532.6   942.2   996.4   996.3   944.7   622.8
  30 -66.667      20.0    20.0    20.0    20.0   532.8   940.6   996.2   996.0   942.4   616.8
  29 -50.000      50.0    50.0    50.0    52.5   532.9   939.9   996.1   995.9   941.4   613.3
  28 -33.333      50.0    50.0    50.0    52.6   532.9   939.7   996.1   995.9   940.7   604.6
  27 -16.667      50.0    50.0    50.0    52.6   532.9   939.7   996.1   995.9   940.2   588.7


 TEMPERATURE DISTRIBUTION IN THE BILLET

                      1       2       3       4       5       6       7       8       9      10      11      12      13      14
                     15      16      17      18      19      20
                   0.00   15.00   47.13   79.25  143.58  156.18  156.78  163.38  169.98  176.58  186.65  197.28  207.55  217.98
                 228.25  238.68  248.95  259.38  269.65  280.08

   1   0.000      50.0    50.0    50.0    52.6   532.9   939.7   996.1   995.9   940.1   584.9
   2  92.586      50.0    50.0    50.0    52.6   533.1   939.9   996.2   996.0   940.3   585.0
   3 185.000      50.0    50.0    50.0    53.4   765.6  1049.5  1089.2  1088.1  1039.7   714.3
   4 203.627      50.0    50.0    50.0    53.2   709.0  1003.7  1051.9  1054.1  1051.5  1015.0   625.9
   5 242.753      50.0    50.0    50.0    53.1   685.0   988.3  1033.0  1035.5  1035.3  1034.0  1007.6   606.4
   6 280.000      50.0    50.0    50.0    53.1   673.2   976.9  1022.2  1024.9  1024.8  1024.6  1023.7   996.0   596.0
```

FIGURE B-9a. PARTIAL SAMPLE OUTPUT FROM RFTEMP FOR THE INPUTS SHOWN IN FIGURES B-5 AND B-8 (Detailed Heat Transfer Analysis)

RESULTS FROM APPROXIMATE HEAT TRANSFER ANALYSIS		
APPROXIMATE TEMPERATURE OF THE DEFORMATION ZONE,C=		.111532E+04
HEAT GENERATED IN THE DEFORMATION ZONE,J	=	.288642E+08
HEAT LOSS TO MANDREL ,J	=	.516775E+06
HEAT LOSS TO ATMOSPHERE VIA CONVECTION,J	=	.592508E+05
HEAT LOSS TO ATMOSPHERE VIA RADIATION ,J	=	.118823E+07
HEAT ABSORBED BY DEFORMING MATERIAL ,J	=	.190999E+08

FIGURE 9b. SAMPLE OUTPUT AFTER SIMPLIFIED HEAT TRANSFER ANALYSIS

The following data cards should not be included in the input data stream, if the third variable (C) in the input list to RFORGE is set to FALSE (F).

8. Eighth Data Card, Format (I10)

Columns 1-10: AS, Number of inlet angles on the die face (3)

9. Ninth Data Card, Format (8F10.4)

Columns 1-80: AT, Die entrance angles. Each angle, beginning from the entrance side, within ten columns, degrees (20., 15., 5.)

Note: Exclude the die land. Continue on an additional card, if AS > 8.

10. Tenth Data Card, Format (8F10.4)

Columns 1-90: AU, Length of each angular segment. Each length beginning from the entrance side, within ten columns, mm (150., 225., 30.)

Note: Exclude the die land. Continue on an additional card, if AS > 8.

As an example, the input data, as printed by the program RFCOMP, are given in Figure B-10. The sample output for the same input data is given in Figure B-11.

DESCRIPTION OF RADFLW AND ASSOCIATED SUBPROGRAMS

This set of computer programs determines a kinematically-admissible upper-bound velocity field, strain rates, strains, and an upper bound on the total forging load in radial forging of gun barrels over a stationary mandrel. In these programs, the new international system of units, "Systeme International" (SI), has been used. A general model of the radial forging of tubes, as shown schematically in Figure B-12, is considered. The model consists of the forging and of the sizing zones. The upper-bound method was utilized for analyzing the deformation process. The details of the analysis and the mathematical derivations are given in Appendix D attached to the final report of Phase-I studies.

```
INPUT TO THE PROGRAM RFCOMP

TOTAL NUMBER OF ANGULAR SEGMENTS IN DIE ENTRANCE =        3
NUMBER OF THE FORGING TOOLS                      =     4
FORGING TOOL ENTRANCE ANGLES,DEGREES
   20.00    15.00     5.00
LENGTHS OF ANGULAR SEGMENTS IN DIE,MM
  150.00   225.00    30.00
```

FIGURE B-10. SAMPLE INPUT DATA AS PRINTED BY RFCOMP PRIOR TO PERFORMING COMPUTATIONS

OUTPUT FROM THE PROGRAM RFCOMP

LENGTH OF THE FORGING ZONE,MM = 323.93

LENGTH OF THE SIZING ZONE,MM = 165.00

DISTANCE OF THE NEUTRAL PLANE FROM ENTRANCE,MM = 482.69

OUTSIDE RADIUS AT THE NEUTRAL SURFACE,MM = 176.50

ENVELOPMENT FACTOR OF FORGING TOOLS = 1.00

RADIAL PRESSURE AT THE NEUTRAL SURFACE,MN/SQ.M = 1455.78

DISTANCE Z MM	RADIUS R MM	STRAIN	STRAIN RATE 1/SEC	FLOW STRESS MN/SQ.M	AXIAL STRESS MN/SQ.M	RADIAL PRESSURE MN/SQ.M
0.	.264508E+03	.732322E-01	.412573E+00	.896318E+02	0.	.896318E+02
.344627E+02	.251957E+03	.713099E-01	.520694E+00	.111045E+03	.753978E+01	.103566E+03
.689253E+02	.239413E+03	.369439E-00	.674772E+00	.135538E+03	.172797E+02	.118250E+03
.939253E+02	.232714E+03	.459087E+00	.785322E+00	.149208E+03	.155532E+02	.133658E+03
.118925E+03	.226616E+03	.555187E+00	.924199E+00	.162351E+03	.131252E+02	.149222E+03
.143925E+03	.219317E+03	.654384E+00	.116187E+01	.175039E+03	.977113E+01	.166068E+03
.168925E+03	.212619E+03	.769287E+00	.133411E+01	.189444E+03	.516936E+01	.184275E+03
.193925E+03	.205930E+03	.890134E+00	.164561E+01	.192936E+03	-.810638E+00	.193753E+03
.218925E+03	.199221E+03	.102302E+01	.207675E+01	.192936E+03	-.853254E+01	.201469E+03
.243925E+03	.192622E+03	.117084E+01	.269729E+01	.192936E+03	-.186475E+02	.211583E+03
.268925E+03	.186023E+03	.133791E+01	.363631E+01	.192936E+03	-.322847E+02	.225221E+03
.293925E+03	.179125E+03	.153876E+01	.515496E+01	.192936E+03	-.515520E+02	.244488E+03
.323925E+03	.176500E+03	.161954E+01	.631703E+01	.192936E+03	-.192200E+03	.395136E+03
.353925E+03	.176500E+03	.161954E+01	.631705E+01	.192936E+03	-.395667E+03	.590667E+03
.378925E+03	.176500E+03	.161954E+01	.631705E+01	.192936E+03	-.772681E+03	.965537E+03
.403925E+03	.176500E+03	.161954E+01	.631705E+01	.192936E+03	-.125423E+04	.145578E+04
.428925E+03	.176500E+03	.161954E+01	.631705E+01	.192936E+03	-.118046E+04	.135374E+04
.453925E+03	.176500E+03	.161954E+01	.631705E+01	.192936E+03	-.506401E+03	.773337E+03
.478925E+03	.176500E+03	.161954E+01	.631705E+01	.192936E+03	-.193467E+03	.386403E+03
.498925E+03	.176500E+03	.161954E+01	.631705E+01	.192936E+03	0.	.192936E+03

TOTAL ROTARY FORGING LOAD (PER TOOL), N = .519274E+06

AVERAGE ROTARY FORGING PRESSURE,MN/SQ.M. = .334228E+03

RADIAL LOAD FOR FORGING (PER TOOL) ,N = .187974E+06 36.18 PERCENT OF TOTAL LOAD

RADIAL LOAD FOR SIZING (PER TOOL) ,N = .331488E+06 63.82 PERCENT OF TOTAL LOAD

FORGING POWER PER TOOL,KW = .934693E+04

FIGURE B-11. SAMPLE OUTPUT FROM RFCOMP FOR THE INPUTS GIVEN IN FIGURES B-5 and B-10

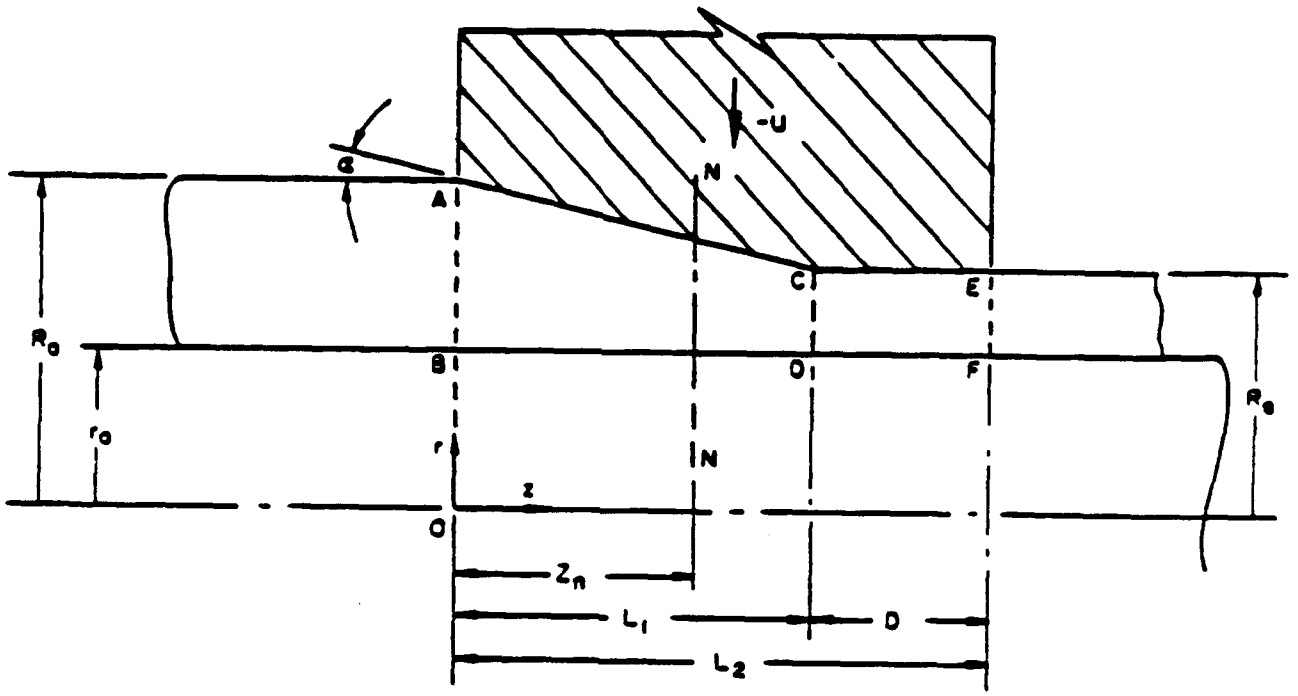

FIGURE B-12. SCHEMATIC DIAGRAM OF RADIAL FORGING OF GUN BARRELS (WITHOUT SINKING ZONE)

Input to and Output from Program RADFLW

The computer program RADFLW uses as input the process variables read by RFORGE. In addition, RADFLW reads in the data required for grid formation.

The computer program RADFLW computes the following quantities:

(1) Length of the forging zone
(2) Distance of the neutral plane from the die entrance
(3) Average strain and average strain rate
(4) Average flow stress
(5) Total radial forging load per tool
(6) Energy rate supplied by a forging tool
(7) The velocity and strain-rate distribution.

The program RADFLW is also applicable to the radial forging of rounds. For this purpose, it is necessary to simply specify the diameter of the mandrel and the friction at the tube mandrel interface as zero.

Details of RADFLW and Other Subprograms

The basic functions of the routine RADFLW and the associated subprograms are briefly described below.

Subroutine RADFLW

This subroutine serves essentially as a coordinating routine. It collects the input data, calls other subprograms, performs some simple arithmetic conversions, and prints out the final results of the upper-bound analysis.

Function ENERGY

Purpose: For a given value of the distance (z_n) of the neutral plane from the die entrance, this subprogram determines the total energy rate of the process. This consists of the power of plastic deformation, the power to overcome frictional constraints, and the shear work rate at the boundaries of velocity discontinuities.

Function Reference: POWER = ENERGY (ZN)

Input: ZN is the distance of the neutral plane from the die entrance.

Variables Transferred through COMMON*: ALFA, AL1, AL2, CFRICD, CFRICM, DVEL, PAI, RE, RM, RN, RO, TALFA

Called By: SIMPLE

Subroutine GSYST

Purpose: This subroutine establishes an orthogonal rectangular grid system over an axial cross section. GR(I) and GZ(J) give the radial and the axial grid lines, and VOL(I,J) are the volumes of each ring element. The elements on the tapered portion of the tool are of triangular cross section.

Calling Sequence: CALL GSYST

Variables Transferred through COMMON: GR, GZ, IEND, JEND, NR, NREXT, NZ, PAI, RE, RM, RN, RO, VOL

Called by: RADFLW

Subroutine SIMPLE

Purpose: This subroutine determines the optimum value of the unknown parameter z_n (distance of the neutral plane from entrance) by minimizing the total energy rate of the process. A simplex method for function minimization is used.

Calling Sequence: CALL SIMPLE (X,N,ALPA,BETA,GAMA,XX,ELIMIT,LIMIT,NPR)

Input: N = the number of independent variables

X = (N+1) sets of initial guesses of independent variables

ALPA = reflection coefficient, a positive constant, less than 1

BETA = contraction coefficient, a positive constant, less than 1

GAMA = expansion coefficient, a positive constant, greater than 1

ELIMIT = error limit on output XX

LIMIT = a limit on the number of iterations

NPR = a printing code during minimization, 1 for yes, 0 for no.

* Variables in the COMMON are described at the end of this appendix.

Output: XX = an array of optimum independent variables.

Calling Routines: ENERGY

Called By: RADFLW

Subroutine MATERL

Purpose: This subroutine furnishes the tabulated flow stress data for a range of strains, strain rates, and temperatures. It also calculates the flow stress for given values of strain, strain rate, and temperature.

Calling Sequence: CALL MATERL (STRAIN, STRRAT, TEMP, FSTRES)

Input: STRAIN = strain, STRRAT = strain rate, TEMP = temperature

Output: FSTRES = flow stress

Variables Transferred through COMMON: DENSTY, SPHEAT

Calling Routines: FSTRS

Called By: FLOW, RADFLW, RFCOMP, RFORLD, TDEFOM

Function FSTRS

Purpose: Using the flow-stress data available from the subroutine MATERL, this subprogram performs the interpolation for determining the flow stress for given values of strain, strain rate, and temperature, which are also supplied by the subroutine MATERL.

Function Reference: FSTRES = FSTRS (MSTRN, MTEMP, T, ASTR, AC, AM, TEMP, STR, STRRAT)

Input: TEMP = temperature, STR = strain, STRRAT = strain rate. The other variables MSTRN, MTEMP, T, ASTR, AC, and AM are internally defined within the subroutine MATERL.

Calling Routines: AITKN

Called By: MATERL

Subroutine AITKN

Purpose: This subroutine performs polynomial interpolation of a table of values Y versus X.

Calling Sequence: CALL AITKN (X, Y, N, K, XB, YB, T, IEX)

Input: X = a one-dimensional array of monotonous independent variable

Y = a one-dimensional array of dependent variables

N = the number of X-Y pairs

K = the degree of interpolating polynomial, $K \leq N - 1$

XB = the value of the independent variable to be used

Output: YB = the interpolated value of the dependent variable

IEX = integer for error check, 1 if extrapolation was performed, 0 otherwise.

The variable name T represents a one-dimensional array of at least 2 (K+1) words used for temporary storage.

Called By: FSTRS, RFCOMP

DESCRIPTION OF RFTEMP AND ASSOCIATED SUBPROGRAMS

RFTEMP and the associated routines are used to obtain temperature distributions in the billet, the mandrel, the die, and the product in radial forging of tubes. The temperature analysis used in developing these programs utilizes a finite-difference algorithm. The numerical procedure approximates the heat generation and the heat transportation during a time interval taking place instantaneously followed by the simultaneous heat conduction during the same time interval. The repetition of these two steps simulates numerically the deformation process and gives the temperature distribution as a function of time. The detailed derivations of the mathematical equations used in these programs are given in Appendix B, attached to the final report of Phase-II studies. A brief description for RFTEMP and its associated subroutines are included later in this appendix.

Input to and Output from RFTEMP

The process variables read by RFORGE are used by RFTEM. All the velocity-related data generated by RADFLW are read from a storage file. In addition, RFTEMP reads in:

(a) Initial uniform temperatures in the die, the mandrel, the coolant and the atmosphere

(b) Billet length and mandrel length

(c) Number of grid lines in the billet, die, and mandrel

(d) Thickness of the scale between mandrel and tube

(e) Fraction of the stroke during which tool keeps contact with the material.

The printout from RFTEMP is in the form of tables which include variables as read in, the velocity-related data and temperatures in the billet, mandrel and die at various time intervals. The temperatures are also printed at the end of the simulation.

Details of RFTEMP and Other Subprograms

The basic functions of RFTEMP and the associated subprograms are described below.

Subroutine RFTEMP

In addition to monitoring the execution of its associated routines, this subroutine reads the process variables, prints all the input information with appropriate captions for the purpose of verification, and reads the velocity-related data. It modifies the velocity field to suit the units in temperature program and prints with suitable captions.

Subroutine COEFF

Purpose: This subroutine calculates the necessary parameter values for heat-transfer calculations.

Calling Sequence: CALL COEFF (No formal parameters)

Variables Transferred through COMMON: AMBTEM, BILLEN, BILTEM, CLEAR2, COLTEM, DELTAZ, DELZ, DIETEM, FRAC, GRX, IBDIE, IEDIE, MANLEN, MANTEM, MAXL, MAXLM1, MAXLP1, MDIE, MPRD, MPRDM1, MPRDP1, MTOT, MTOTM1, MTOTP1, NBIL, NDIE, NDIEM1, NDIEP1, NMAN, NMANM1, NMANP1, NMANT, NRDL, NTOT, NTOTP1, NZ, NZTEMP, RTEMP, R1, R2, R21, R3, R32, R4, R43, SURT, T, TSCR and Z.

Called By: RFTEMP

Subroutine FORGNG

Purpose: Based on stability criterion, this subroutine estimates the critical time interval, Δt, for compiling temperatures by the finite-difference method. In addition, FORGNG calculates such quantities as the instantaneous billet volume, volume of metal trapped in the deformation zone, product volume, and the number of steps required to move the billet by one grid length.

Calling Sequence: CALL FORGNG

Variables Transferred through COMMON: AKA, AKB, AKD, AKM, BILIR, BILOR, BILVEL, CANG, CLEAR2, COLTEM, CONST, CONVOL, CRA, CRB, CRD, CRM, DELT, DELTAZ, DELZ, DIETEM, FRAC, GRX, GRY, HTCB, HTCD, HTFD, IEDIE, IPRINT, ITESIM, JTEMP, KJ, LIMIT, MAXL, MBPROD, MDIF, MEPROD, MNPRDO, MNPROD, MPRD, MTOT, NBBIL, NBILT, NCONT, NDIE, NDIEM1, NDIEP1, NDOASN, NEBIL, NMAN, NMANP1, NMANT, NRDL, NSTRK, NTOT, NZTEMP, IP, POWER, RTEMP, R1, R21, R32, R4, R43, SURT, T, TFRAC, TSCR, TUBIR, TUBOR, VR, VZ, Z.

Calling Routines: AIR, BILLET, DIE, FRGTEM, MANDL, RFORLD, TDEFOM, TPRINT

Called By: RFTEMP

Subroutine FRGTEM

Purpose: FRGTEM estimates the temperature distribution after heat transfer during radial-forging operation.

Calling Sequence: CALL FRGTEM

Variables Transferred through COMMON: AKA, AKB, AKD, AKM, AMBTEM, CLEAR2, CLEAR4, COLTEM, CRA, CRB, CRD, CRM, DELT, DELTAZ, DELZ, FRAC, HTCB, HTCD, HTCM, HTFB, HTFD, IBDIE, IEDIE, IPRINT, KJ, MAXL, MEPROD, MNPROD, MPRD, MTOT, NBBIL, NCONT, NDIE, NEBIL, NMANT, NTOT, NZTEMP, RTEMP, R1, R21, R32, R4, R42, R43, SURT, T, TSCR

Calling Routines: AIR, BILLET, DIE, MANDL

Called By: FORGNG

Subroutine SIMPHT

Purpose: SIMPHT estimates by simplified approximate equations, (a) average temperature of the deformation zone at the end of the process, (b) heat gained due to metal deformation, (c) heat lost to atmosphere by convection, (d) heat lost to atmosphere by radiation, and (e) heat lost to mandrel by heat conduction.

Calling Sequence: CALL SIMPHT

Variables Transferred through COMMON: AKD, AMBTEM, BILOR, BILTEM, BILVEL, COLTEM, CRB, DI, DLAND, DO, MANTEM, PI, POWER, PRESSR, TANG, TUBIR, TUBOR

Calling Routines: BILLET, MANDL

Called By: RFTEMP

Subroutine TDEFOM

Purpose: TDEFOM calculates the temperature gain due to plastic deformation of the billet material.

Calling Sequence: CALL TDEFOM

Variables Transferred through COMMON: AMBTEM, BILOR, BILVEL, CFRICD, CFRICM, CRB, CRD, CRM, DELT, DELTAZ, DELZ, DLAND, ENVLOP, GRX, GRY, IBDIE, IEDIE, IPRINT, KJ, MAXL, MEPROD, MNPROD, MPRD, MTOT, NBBIL, NCONT, NDIE, NEBIL, NMANT, NRDL, NZTEMP, RTEMP, STRAIN, STRRAT, SURT, T, TSCR, TUBIR, TUBOR, TUBVEL, VR, and VZ

Calling Routines: BILLET, DIE, MANDL, MATERL

Called By: FORGNG

Subroutine RFORLD

Purpose: Calculates the radial-forging load per tool.

Calling Sequence: CALL RFORLD

Variables Transferred through COMMON: ALOAD, CFRICD, CFRICM, CLEAR2, CONVOL, DELTAZ, DVEL, NBBIL, NDIE, NMANT, NRDL, NZTEMP, PI, POWER, RTEMP, STRAIN, STRRAT, TSCR, TUBIR, TUBOR, and VZ

Calling Routines: MATERL

Called By: FORGNG

Subroutine AIR

Purpose: Defines the thermal properties for the atmospheric air.

Calling Sequence: CALL AIR(TEMP)

TEMP: Temperature of the air

Variables Transferred through COMMON: AKA, CRA

Called By: FORGNG, FRGTEM

Subroutine BILLET

Purpose: Defines the thermal properties for the billet material.

Calling Sequence: CALL BILLET(TEMP)

TEMP: Average temperature of the billet

Variables Transferred through COMMON: AKB, CRB, HTCB, HTFB

Called By: FORGNG, FRGTEM, SIMPHT, TDEFOM

Subroutine DIE

Purpose: Defines the thermal properties for the die material.

Calling Sequence: CALL DIE(TEMP)

TEMP: Average temperature of the die

Variables Transferred through COMMON: AKD, CRD, HTCD, HTFD

Called By: FORGNG, FRGTEM, TDEFOM

Subroutine MANDL

Purpose: Defines the thermal properties for the mandrel material.

Calling Sequence: CALL MANDL (TEMP)

TEMP: Average temperature of the mandrel

Variables Transferred through COMMON: AKM, CRM, HTCM, HTFM

Called By: FORGNG, FORTEM, SIMPHT, TDEFOM

In addition, RFTEMP utilizes subprograms MATERL, FSTRS, and AITKN described under RADFLW.

DESCRIPTION OF RFCOMP AND ASSOCIATED SUBPROGRAMS

The computer program RFCOMP determines the quantitative relationships between various process variables in radial forging of gun barrels, or tubes, using the compound-angle dies (multiple angles on the die entrance). In its present structure, RFCOMP can consider up to nine different angles on the die entrance and is applicable to both the round-faced and the flat-faced forging tools. A general model of radial forging of tubes, as shown in Figure B-13 with three entrance angles, is considered. This model consists of the forging and the sizing zones. The slab method was utilized for analyzing the deformation mechanics.

The program RFCOMP is also applicable to the radial forging of rounds. For this purpose, it is necessary to simply specify the inside diameter of the billet, the diameter of the mandrel, and the friction at the tube-mandrel interface as zero.

Input to and Output from RFCOMP

In addition to the process variables read by RFORGE, RFCOMP uses as input:

(a) Number of angular segments in the dies

(b) Entrance angles, degree

(c) Lengths of angular segments in dies, mm

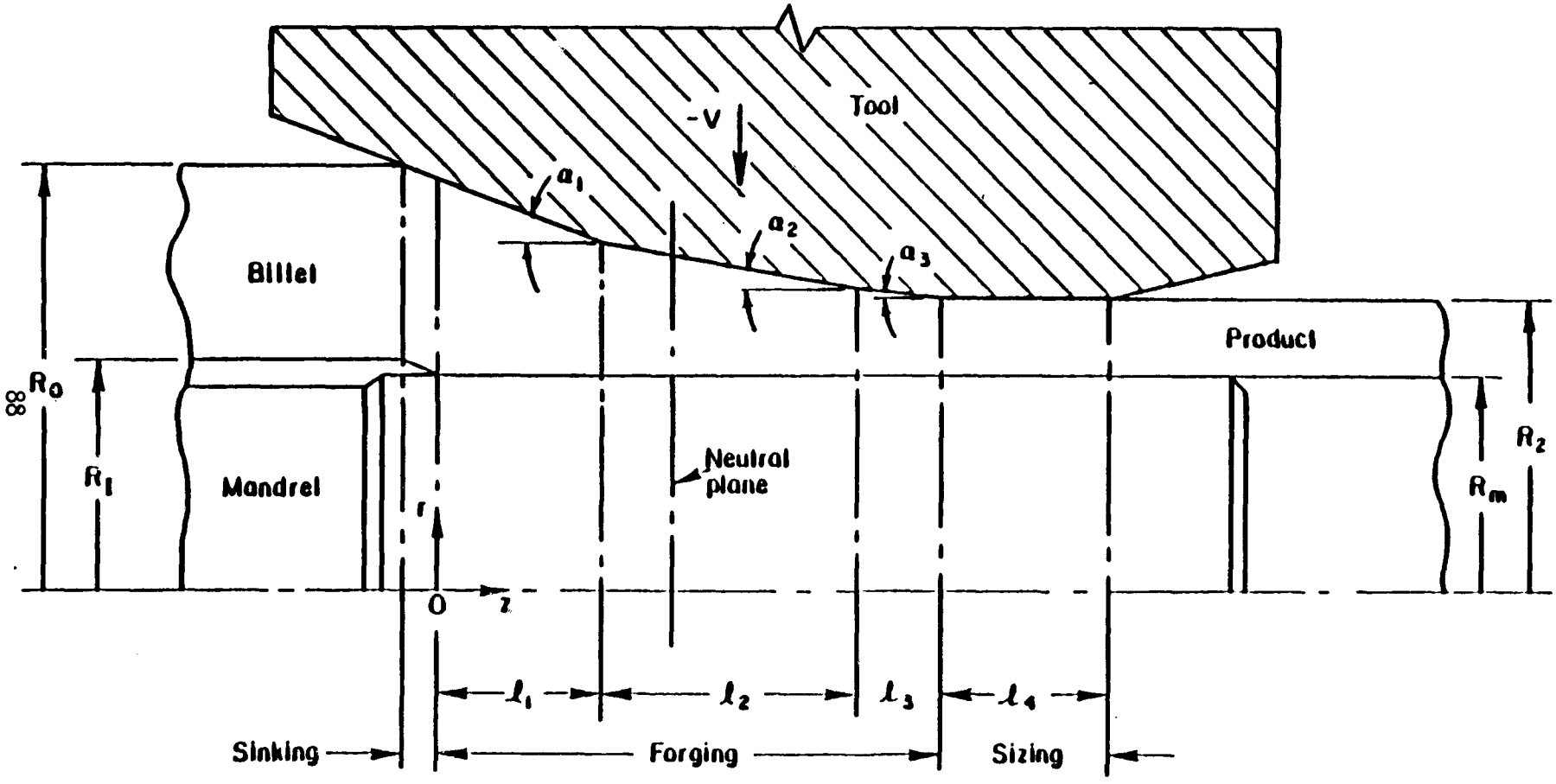

FIGURE B-13. GENERAL MODEL OF RADIAL FORGING OF GUN TUBES WITH COMPOUND-ANGLE DIES

The computer program RFCOMP computes the following quantities:

(a) Lengths of the forging and the sizing zones
(b) Distance of the neutral plane from the die entrance
(c) Strain, strain rate, flow stress, axial stress, and the radial pressure distribution along the axis in the deformation zone
(d) Total radial-forging load
(e) Average radial forging pressure
(f) Components of the total load in the form of forging and sizing loads

Details of RFCOMP and the Associated Subprograms

The basic functions of RFCOMP and the various subprograms of RFCOMP are briefly described below.

Subroutine RFCOMP

This routine serves essentially as a coordinating routine. It collects the input data, calls other subprograms, performs some simple arithmetic conversions, and prints out the final results of the stress and load analysis.

Subroutine PRESUR

Purpose: This subroutine generates the radial pressure and the axial stress distributions starting from either end of the deformation zone. The intersection of the two pressure curves, thus generated, gives the location of the neutral plane and minimum of the two values of the calculated radial pressure is taken as the actual pressure.

Calling Sequence: CALL PRESUR (ICALL)

Input: ICALL is either 1 or 2. When ICALL = 1, the subroutine PRESUR is called in order to determine the neutral plane. When ICALL = 2, it is called for determining the actual radial pressure distribution.

Variables Transferred through COMMON: ALFA, BPULL, CFRICD, CFRICM, DLAND, FPULL, FSTR, FSTRES, NFORG, NSTEP, PRL, PRR, R, RI, R2, STR, STRAIN, STRR, STRRAT, SZL, SZR, TL, T1, Z

Calling Routines: FLOW

Called By: RFCOMP

Subroutine FLOW

Purpose: At a given radial plane in the deformation zone, this subroutine calculates the strain, the strain rate, and it determines the flow stress by calling the subroutine MATERL.

Calling Sequence: CALL FLOW (ZZ, RR)

Input: ZZ is the distance of a given radial plane from the die entrance, and RR is the outside radius at that location.

Variables Transferred through COMMON: DLAND, DVEL, FSTRES, RI, RM, RN, RO, R2, STRAIN, STRRAT, TEMPR, TL

Calling Routine: MATERL

Called By: PRESUR, RFCOMP

In addition, RFCOMP utilizes the subprograms MATERL, FSTRS, and AITKN described under RADFLW.

TABLE B-1. CROSS REFERENCE TABLE FOR SUBPROGRAM CALLINGS

	Calling	Called By
1. AIR		FORGNG,FRGTEM
2. AITKN		FSTRS,RFCOMP
3. BILLET		FORGNG,FRGTEM,TDEFOM
4. COEFF		RFTEMP
5. DIE		FORGNG,FRGTEM,TDEFOM
6. ENERGY		SIMPLE
7. FLOW	MATERL	PRESUR,RFCOMP
8. FORGNG	AIR,BILLET,DIE,FRGTEM,MANDL, RFORLD,TDEFOM,TPRINT	RFTEMP
9. FRGTEM	AIR,BILLET,DIE,MANDL	FORGNG
10. FSTRS	AITKN	MATERL
11. GSYST		RADFLW
12. MANDL		FORGNG,FRGTEM,TDEFOM
13. MATERL	FSTRS	FLOW,RADFLW,RFCOMP,RFORLD, TDEFOM
14. PRESUR	FLOW	RFCOMP
15. RADFLW	GSYST,MATERL,SIMPLE	RFORGE
16. RFCOMP	AITKN,FLOW,MATERL,PRESUR	RFORGE
17. RFORGE	RADFLW,RFCOMP,RFTEMP	
18. RFORLD	MATERL	FORGNG
19. RFTEMP	COEFF,FORGNG	RFORGE
20. SIMPHT	BILLET,MANDL	RFTEMP
21. SIMPLE	ENERGY	RADFLW
22. TDEFOM	BILLET,DIE,MANDL,MATERL	FORGNG
23. TPRINT		FORGNG

TABLE B-2. LIST OF VARIABLES PRINTED FOR DIFFERENT SETTINGS OF IPRINT

The following variables will be printed when IPRINT is set higher or equal to the value shown below.

Value of IPRINT	Variables Listed
0	(a) All error messages
	(b) DO,DI,DE,DM,DVEL,AXFEED,DIEANG,BPULL, FPULL,CFRICD,CFRICM,BILTEM,PHI,SAI, and ITOOL from RFORGE
	(c) CF,DLAND,ZN,RN,ENVLOP, and PN from RFCOMP
	(d) ZN,RN,STRAIN,STRRAT,FSTRES,SN,PN, ALOAD,ANGPR,FORGL,PCFORG,SIZEL,PSIZE, and POWER from RFCOMP
	(e) Temperature distribution in the billet, the die, the mandrel and the product at the beginning, at times when billet moves through one grid line distance, and at the end of iterations from RFTEMP
1	(a) VELCTY,TMPRTR,PRESSR,IPRINT from RFORGE
	(b) NR,NZ,NREXT from RADFLW
	(c) ALL,ZN,STRAIN,STRRAT,FSTRES,ALOAD,PRESUR, TFIN, and TWORK from RADFLW
	(d) DPIPE,MANLEN,BILLEN,STROKE,AMBTEM,DIETEM, MANTEM,COLTEM,NBILT,NMANT,MDIE,LIMIT, SCALE, and TFRAC from RFTEMP
	(e) NANGLE from RFCOMP

2	(a)	ALFA(J),AL(J) J = 1, NANGLE from RFCOMP
3	(a)	I,J,GZ(J),GR(I),UZ(I,J),UR(I,J),SR(I,J) for I = 1 to IEND(J) and J = 1 to NZP1 from RADFLW
	(b)	NRDL,MAXL,NZ(J) J = 1 to NRDL from RFTEMP
	(c)	J,Z(J),VZ(I,J),VR(I,J),STRAIN(I,J), and STRRAT(I,J) for I = 1 to NZ(J) and J = 1 to NRDL from RFTEMP
4	(a)	I,J,KUP,KDN,KRG,KLF,CEQ,CONST, and CHECK for I = 1 to MTOT and J = 2 to NTOTM1 from FORGNG
	(b)	K,I,T(I,1),T(I+1,1),T(I,MBPROD) for K = 1 to NDO and I = 1 to NZ(K) from FORGNG
	(c)	I,J,KUP,KDN,KRG,KLF,CEQ,TZ1,+Z2,TS,TUP, TDN,TRG,TLF,TSCR(I,J),T(I,J) for I = 1 to MTOT and J = NBBIL to JEND from FRGTEM
	(d)	TRISE for J = 1 to NDIE and I = NMANT to NZ(J) from TDEFOM

Description of the Variables in the COMMON Statements

Most of the important variables are transferred between subroutines through COMMON statements, named ARRY and SCLR. For easy reference, all the variables in the COMMON statements are described below in alphabetical order.

AKA	Thermal conductivity of air
AKB	Thermal conductivity of billet material
AKD	Thermal conductivity of die material
AKM	Thermal conductivity of mandrel material
AL	Lengths of angular segments on the die face with multiple angles
AL1	Length L_1 in Figure B-5
AL2	Length L_2 in Figure B-5
ALFA	Die angle. Angle α in Figure B-5
ALFA	Array of angles (in RFCOMP and associated routines)
ALOAD	Forging load per tool
AMBTEM	Ambient temperature
AR	Outside radius at the beginning of each angular segment
AXFEED	Axial feed of the billet per stroke
BILLEN	Billet length
BILOR	Billet outer radius
BILTEM	Billet temperature
BILVEL	Billet velocity
BPULL	Back-pull force (with a negative sign if back push)
CANG	Cosine of the die angle
CFRICD	Friction shear factor at the die surface
CFRICM	Friction shear factor at the mandrel surface
CL	Axial distances of starting points of each angular segment
CLEAR2	One-half of the clearance between billet inner radius and tube inner radius
CLEAR4	One-fourth of the clearance between billet inner radius and tube inner radius

COLTEM	Temperature of the coolant in the mandrel
CONVOL	Volumes of ring elements in the deformation zone
CRA	Product of specific weight and heat capacity of air
CRB	Product of specific weight and heat capacity of billet material
CRD	Product of specific weight and heat capacity of die material
CRM	Product of specific weight and heat capacity of mandrel material
DE	Outside diameter of the forged product
DELT	Delta T. Time interval Δt for heat transfer calculations
DELTAZ	Delta Z. Axial distance between two successive radial grid lines
DELZ	Similar to DELTAZ but has a fixed value which is the axial distance between two successive radial grid lines in the billet outside the deformation zone
DENSTY	Density of the material
DI	Inside diameter of the tubular preform
DIEANG	Die angle
DIETEM	Die temperature
DLAND	Die land length
DM	Inside diameter of the forged product or diameter of the mandrel
DO	Outside diameter of the tubular preform
DVEL	Radial velocity of hammers
DZ	Delta Z in each angular segment
ENVLOP	Envelopment factor of the forging tool
FPULL	Front-pull force (with a negative sign if front push)
FR	Strain rates/area at neutral plane
FRAC	Have values equal to $R_i/\Delta R_i$ where R_i = [RTEMP(I) + RTEMP(I-1)]/2 ΔR_i = RTEMP(I) - RTEMP(I-1)

FSTR	Array of flow stresses
FSTRES	Average flow stress in the material
GR	Radial coordinates of grid points
GRX	Axial distances of successive radial grid lines starting from the exit of the die
GRY	GRY(J) is the surface area at the die-billet interface at grid Point J
HTCB	Heat transfer coefficient at the cylindrical surface of the billet material
HTCD	Heat transfer coefficient at the cylindrical surface of the die material
HTCM	Heat transfer coefficient at the cylindrical surface of the mandrel material
HTFB	Heat transfer coefficient at the flat surface of the billet material
HTFD	Heat transfer coefficient at the flat surface of the die material
HTFM	Heat transfer coefficient at the flat surface of the mandrel material
IBDIE	Subscript of the radial grid line with which die back section begins
IEDIE	Subscript of the radial grid line with which die back section ends. Both IBDIE and IEDIE refer the storage locations.
IEND	Number of radial divisions at an axial location inside the dies
IPRINT	Intermediate results are being printed when IPRINT is set a value between 0 to 5. Refer to Table B-2, page B-33.
ITESIM	Maximum allowed number of iterations during metal deformation
ITOOL	A code number for type of tool (1 for round and 2 for flat face)
JEND	Number of axial divisions at a radial location inside the dies
JTEMP	Has a value equal to IEDIE + 1 and is used by TPRINT for printing purposes

KJ	An index to indicate finish shape product has begun coming out
LIMIT	Subscript of the radial grid line at which when the billet end reaches, the process simulation is to be stopped. For example, if NDIE is equal to 10 and NBILT is equal to 20, the billet end will be at (10 + 20 =) 30th radial grid line. To stop the process when one-half of the billet length is forged, LIMIT must be set to (10 + 10 =) 20. To forge the complete length of the billet LIMIT must be 10. To forge the billet through only one grid length distance LIMIT must be equal to 29.
MANLEN	Mandrel length. Note: real variable
MANTEM	Mandrel temperature. Note: real variable
MAXL	Number of axial grid lines from the center of the mandrel to the outer surface of the billet
MAXLM1	MAXL minus one
MAXLP1	MAXL plus one
MBPROD	Subscript of the radial grid line at which product begins to emerge
MDIE	Number of axial grid lines in the die above the billet outer surface
MDIFF	Number of radial grid lines by which the temperature distribution in the mandrel is shifted with respect to the temperature distribution in the billet at the end of each cycle in order to compensate for the relative velocity between the billet and mandrel
MEPROD	Subscript of the radial grid line with which product front face coincides. (Similar to IBDIE and IEDIE, MBPROD and MEPROD refer to the storage locations).

MNPRDO	MNPROD old. The value of the MNPROD in the previous cycle is stored in this variable
MNPROD	Difference between MEPROD and MBPROD
MPRD	Number of axial grid lines in the product
MPRDM1	MPRD minus one
MPRDP1	MPRD plus one
MTOT	Total number of axial grid lines including the die
MTOTM1	MTOT minus one
MTOTP1	MTOT plus one
NANGLE	Number of inlet angles on the die face
NBBIL	Subscript of the radial grid line with which the billet front face coincides at the beginning of a cycle
NBILP1	NBILT plus one
NBILT	Number of radial grid lines in the billet
NCONT	Number of contacts between the die and the material during the calculated time interval, Δt
NDIE	Subscript of the radial grid line with which the entrance face of the die coincide
NDIEM1	NDIE minus one
NDIEP1	NDIE plus one
NDIV	Number of divisions in each angular segment (RFCOMP)
NDOASN	NDO assigned. NDO is the number of cycles used for process simulation. By assigning a value to NDOASN number of cycles used for process simulation can be reduced to a preset value. Useful for program debugging.
NEBIL	Subscript of the radial grid line with which the billet and face coincides at the beginning of a cycle
NFORG	Number of divisions in the forging zone
NMAN	Number of radial grid lines in the mandrel
NMANM1	NMANT minus one
NMANP1	NMANT plus one

NRN	Number of radial divs on exit side of neutral pl.
NMANT	Number of axial grid lines in the mandrel
NR	Number of radial divisions on the entrance side
NRDL	Number of radial grid lines from die exit to billet end surface
NREXT	Number of radial divisions on the exit side
NSTEP	Total number of divisions in the zone of deformation
NSTRK	Number of strokes in the calculated time interval, Δt
NTOT	Total number of radial grid lines
NZ	NZ(J) is the number of axial grid lines at the die surface for the J radial grid line. NZ is read in and then modified to account for the grid lines in the mandrel
NZTEMP	Same as NZ
PAI	Same as PI
PHI	Tool contact angle (for round tools only) Refer to Figure B-2
PI	A constant equal to 3.141592654
POWER	Forging power per tool
PR	Array of radial pressures on the dies
PRESUR	Logical variable to indicate that pressure and load calculations are to be performed
PRL	Array of pressures from the die entrance side
PRR	Array of pressures from the die exit side
R	Radial distances of the axial grid lines as read. The same array is used later to print radial distances in mm units, also outside radius at a given axial location.
RE	Outer radius of the forged product
REDRAT	Area reduction ratio
RFLOAD	Not used
RI	Inner radius of the tubular preform
RM	Inner radius of the forged product or radius of the mandrel

RN	Outside radius at neutral plane
RO	Outer radius of the tubular preform
RPIPE	Radius of the cooling pipe
RTEMP	Modified radial distances of the axial grid lines which accounts for the mandrel radius
R1	A fixed value equal to (RTEMP(NMANP1) + RTEMP(NMANM1))/2
R2	R1 minus CLEAR2 (in RFTEMP and associated subprograms). Same as RE (in RFCOMP and associated subprograms).
R21	$(R2)^2 - (R1)^2$
R3	R1 plus CLEAR2
R32	$(R3)^2 - (R2)^2$
R4	(RTEMP(NMANP1) + RTEMP(NMANT))/2
R42	$(R4)^2 - (R2)^2$
R43	$(R4)^2 - (R3)^2$
SAI	Tool tangency angle (for flat tools only)
SCR	Scratch array for determining AR
SPHEAT	Specific heat of the material
SQ3	A constant equal to the square root of 3
SR	Strain rates at grid points
STR	Array of strains
STRAIN	Strain in the material at each grid point
STROKE	Number of forging strokes per minute
STRR	Array of strain rates
STRRAT	Strain rate in the material at each grid point
SURT	Surface area of the element at the intersection of Ith axial grid line and Jth radial grid line. It is equal to [RTEMP(I) + RTEMP(I - 1)]*[2 x (RTEMP(I) - RTEMP(I - 1))]
SZ	Array of axial stresses
SZL	Array of axial stresses from the entrance side
SZR	Array of axial stresses from the exit side

T	Temperature at the intersection of the Ith axial and Jth radial grid lines
TALFA	Tangent of entrance angle
TALFA	Array of tangents of angles (in RFCOMP and associated routines)
TANG	Tangent of the die angle
TEM	Array of temperatures
TEMP	Average temperature
TERM	Value of energy rate integral in RADFLW
TFRAC	Fraction of the stroke time during which tool and material are in contact
TL	Total die length, equal to $l_1 + l_2 + l_3 + l_4$ in Figure B-10
TMPRTR	Logical variable to indicate that temperature distribution is to be calculated
TO	RO - RI
TSCR	A scratch array used to store intermediate temperature values
TUBIR	Tube inner radius
TUBOR	Tube outer radius
TUBVEL	Tube velocity
UR	Radial velocities at grid points
UZ	Axial velocities at grid points
VELCTY	Logical variable to indicate that velocity field is to be generated
VOL	Volume of elements around grid points
VR	Radial velocity of the element at the intersection of Ith axial and Jth radial grid lines
VZ	Axial velocity of the element at the intersection of Ith axial and Jth radial grid lines
Z	Axial distances of the radial grid lines as read. The same array is used later to print axial distances in mm units.
ZN	Distance of the neutral plane from die entrance.

TECHNICAL REPORT INTERNAL DISTRIBUTION LIST

	NO. OF COPIES
CHIEF, DEVELOPMENT ENGINEERING DIVISION	
ATTN: SMCAR-CCB-DA	1
-DC	1
-DI	1
-DR	1
-DS (SYSTEMS)	1
CHIEF, ENGINEERING DIVISION	
ATTN: SMCAR-CCB-S	1
-SD	1
-SE	1
CHIEF, RESEARCH DIVISION	
ATTN: SMCAR-CCB-R	2
-RA	1
-RE	1
-RM	1
-RP	1
-RT	1
TECHNICAL LIBRARY	
ATTN: SMCAR-CCB-TL	5
TECHNICAL PUBLICATIONS & EDITING SECTION	
ATTN: SMCAR-CCB-TL	3
OPERATIONS DIRECTORATE	
ATTN: SMCWV-ODP-P	1
DIRECTOR, PROCUREMENT & CONTRACTING DIRECTORATE	
ATTN: SMCWV-PP	1
DIRECTOR, PRODUCT ASSURANCE & TEST DIRECTORATE	
ATTN: SMCWV-QA	1

NOTE: PLEASE NOTIFY DIRECTOR, BENÉT LABORATORIES, ATTN: SMCAR-CCB-TL OF ADDRESS CHANGES.

TECHNICAL REPORT EXTERNAL DISTRIBUTION LIST

	NO. OF COPIES
ASST SEC OF THE ARMY RESEARCH AND DEVELOPMENT ATTN: DEPT FOR SCI AND TECH THE PENTAGON WASHINGTON, D.C. 20310-0103	1
ADMINISTRATOR DEFENSE TECHNICAL INFO CENTER ATTN: DTIC-FDAC CAMERON STATION ALEXANDRIA, VA 22304-6145	12
COMMANDER U.S. ARMY ARDEC ATTN: SMCAR-AEE	1
SMCAR-AES, BLDG. 321	1
SMCAR-AET-O, BLDG. 351N	1
SMCAR-CC	1
SMCAR-FSA	1
SMCAR-FSM-E	1
SMCAR-FSS-D, BLDG. 94	1
SMCAR-IMI-I, (STINFO) BLDG. 59 PICATINNY ARSENAL, NJ 07806-5000	2
DIRECTOR U.S. ARMY RESEARCH LABORATORY ATTN: AMSRL-DD-T, BLDG. 305 ABERDEEN PROVING GROUND, MD 21005-5066	1
DIRECTOR U.S. ARMY RESEARCH LABORATORY ATTN: AMSRL-WT-PD (DR. B. BURNS) ABERDEEN PROVING GROUND, MD 21005-5066	1
DIRECTOR U.S. MATERIEL SYSTEMS ANALYSIS ACTV ATTN: AMXSY-MP ABERDEEN PROVING GROUND, MD 21005-5071	1
COMMANDER ROCK ISLAND ARSENAL ATTN: SMCRI-ENM ROCK ISLAND, IL 61299-5000	1
MIAC/CINDAS PURDUE UNIVERSITY P.O. BOX 2634 WEST LAFAYETTE, IN 47906	1
COMMANDER U.S. ARMY TANK-AUTMV R&D COMMAND ATTN: AMSTA-DDL (TECH LIBRARY) WARREN, MI 48397-5000	1
COMMANDER U.S. MILITARY ACADEMY ATTN: DEPARTMENT OF MECHANICS WEST POINT, NY 10966-1792	1
U.S. ARMY MISSILE COMMAND REDSTONE SCIENTIFIC INFO CENTER ATTN: DOCUMENTS SECTION, BLDG. 4484 REDSTONE ARSENAL, AL 35898-5241	2
COMMANDER U.S. ARMY FOREIGN SCI & TECH CENTER ATTN: DRXST-SD 220 7TH STREET, N.E. CHARLOTTESVILLE, VA 22901	1
COMMANDER U.S. ARMY LABCOM MATERIALS TECHNOLOGY LABORATORY ATTN: SLCMT-IML (TECH LIBRARY) WATERTOWN, MA 02172-0001	2
COMMANDER U.S. ARMY LABCOM, ISA ATTN: SLCIS-IM-TL 2800 POWER MILL ROAD ADELPHI, MD 20783-1145	1

NOTE: PLEASE NOTIFY COMMANDER, ARMAMENT RESEARCH, DEVELOPMENT, AND ENGINEERING CENTER, U.S. ARMY AMCCOM, ATTN: BENÉT LABORATORIES, SMCAR-CCB-TL, WATERVLIET, NY 12189-4050 OF ADDRESS CHANGES.